

# Scenarios of superluminous supernovae in radiation hydrodynamics simulations



**Alexey Tolstov (Kavli IPMU)**

**Ken'ichi Nomoto (Kavli IPMU)**

**Sergey Blinnikov (ITEP, Kavli IPMU)**

**Elena Sorokina (SAI MSU)**

**Andrey Zhiglo (NSC KIPT, Kavli IPMU)**

**Robert Quimby (SDSU, Kavli IPMU)**

**Petr Baklanov (ITEP)**

**Alexandra Kozyreva (TAU)**

# Outline

- Observations of SLSNe and possible scenarios
- Extremely bright in UV SLSN  
Gaia16apd ( $M_{UV} \sim -23$  mag)
- Radiation hydrodynamics simulations of SLSN-I outbursts
- Multicolor light curves (from X-rays to NIR), color evolution, photospheric temperature and velocity evolution. The influence of opacity, metallicity of CSM
- Constraints on SLSN-I scenarios

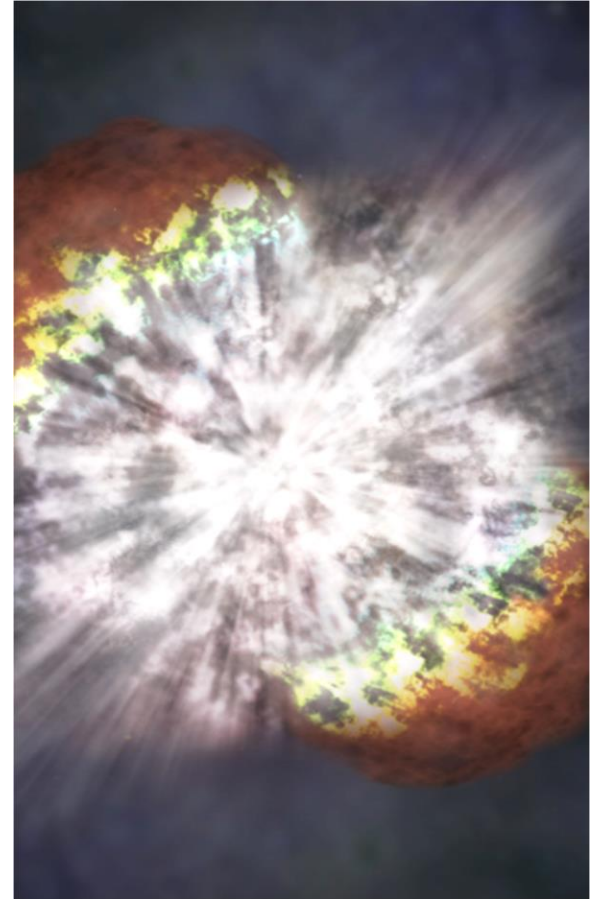


(Image credit: NASA)

# Superluminous supernovae (SLSNe)

- SLSNe (**Type I (no hydrogen)**, **Type II**) are more luminous than -21 magnitude (arbitrary cut) in any optical band at the maximum brightness
- Rise  $\sim 20-70$  d, decline  $\sim 20-500$  d

$$E_{\text{rad}} \sim (1-10) \cdot 10^{51} \text{ erg, rate/CC} \sim 0.01\%,$$

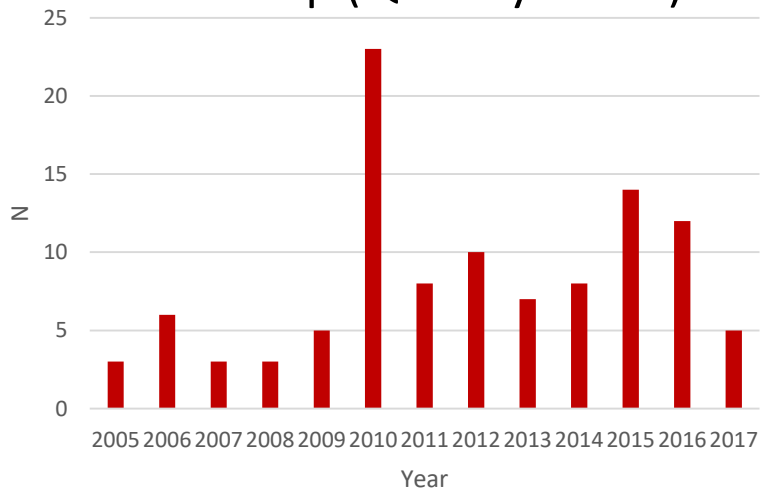
$\sim 100$  SLSNe,  $z \sim 0.1 - 3.9$

(PTF, Pan-STARRS)

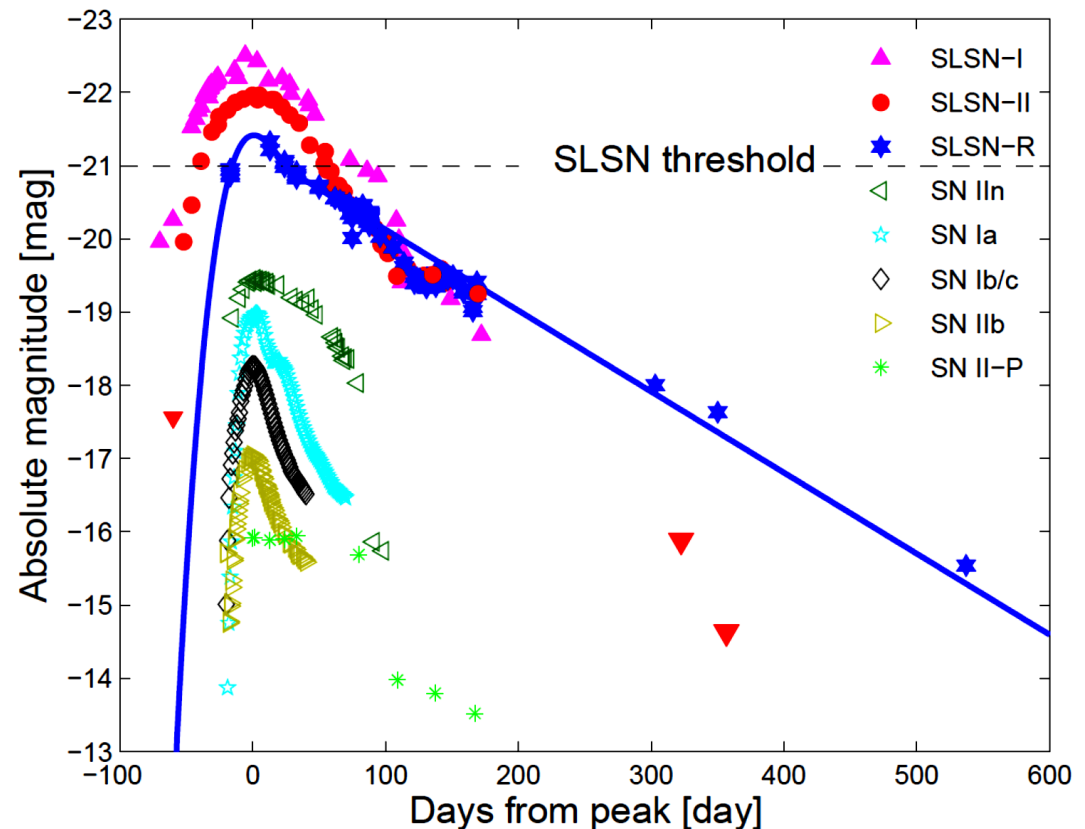
SLSN discoveries:

SN 2006gy (Smith+2007),

SN 2005ap (Quimby+2007)

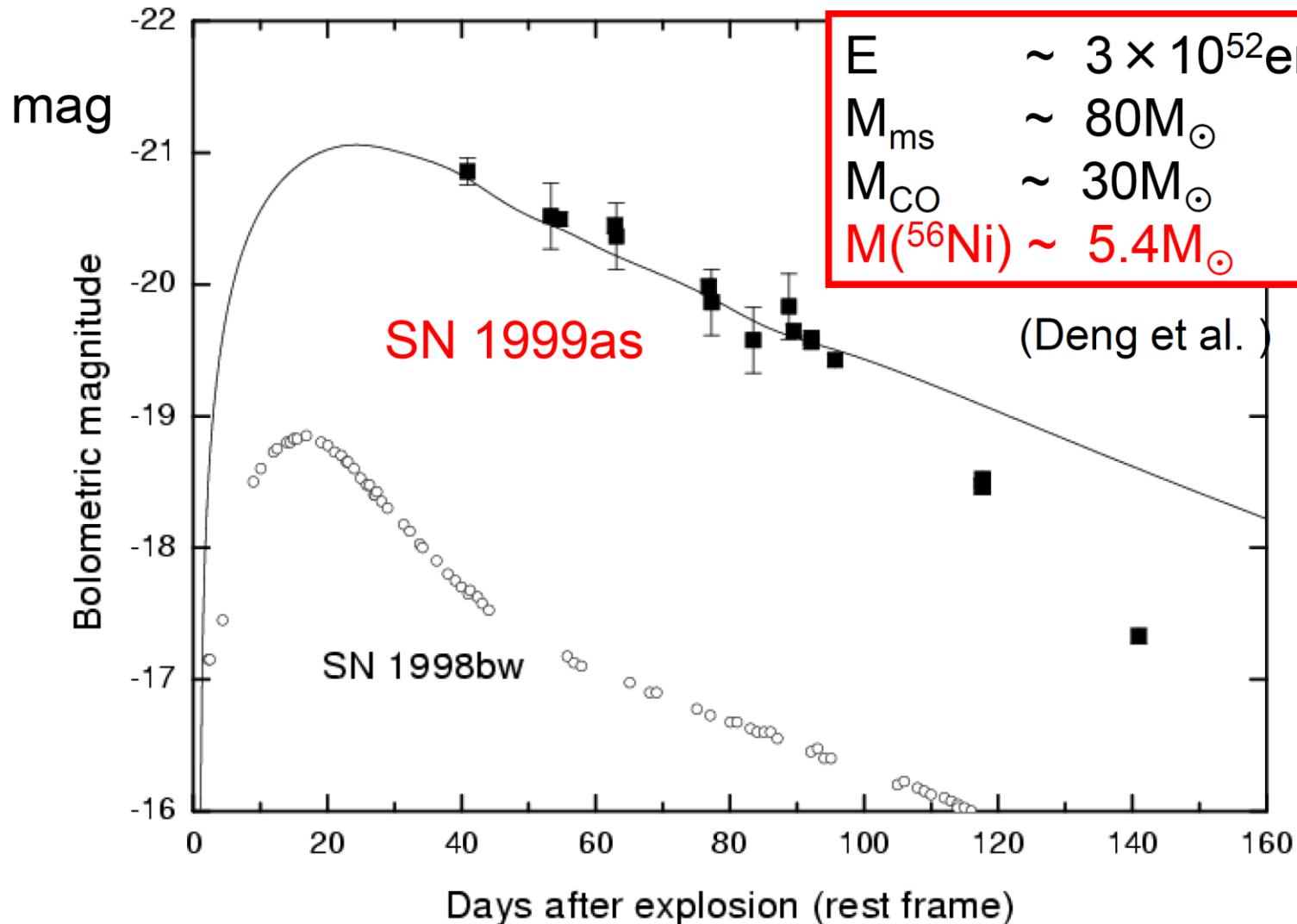


Gal-Yam 2012

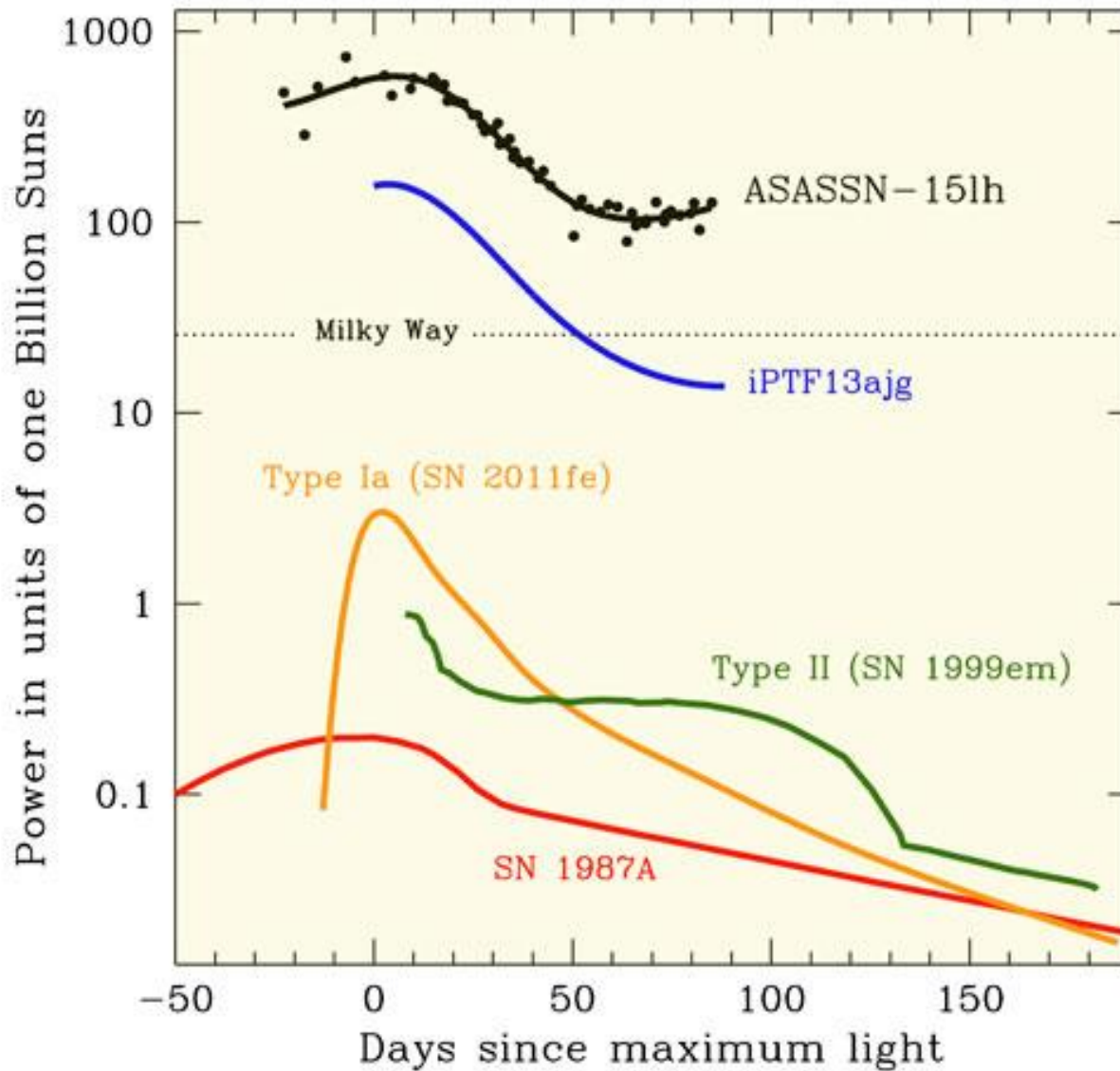


# Superluminous SNe: 1999as @z=0.127

(Knop et al.)



# Most luminous SLSNe



# SLSN subclasses

- Type I (no hydrogen), Type II

## SLSN I normal

Rapid light curve decay (~20-60 d)  
Quimby+2011

## SLSN I-R (SN 2007bi-like)

Exponential light curve decay  
Gal Yam+2009

## SLSN I - fast (PS1-10afx)

Very fast rise and fall (~ 10-20 d)  
Chornock+2013  
Probably a lensed Ia  
Quimby+2013, 2014

## SLSN II-n

Narrow/intermediate H lines,  
rapid rise, but very slow fall (~100 d)

## SLSN II-n-peculiar (SN 2006gy)

Complicated, evolving H profile  
Extremely long-lived (~300 d)

## SLSN II-L (SN 2008es, CSS121025)

Broad H lines only after peak,  
short-lived with fast decay

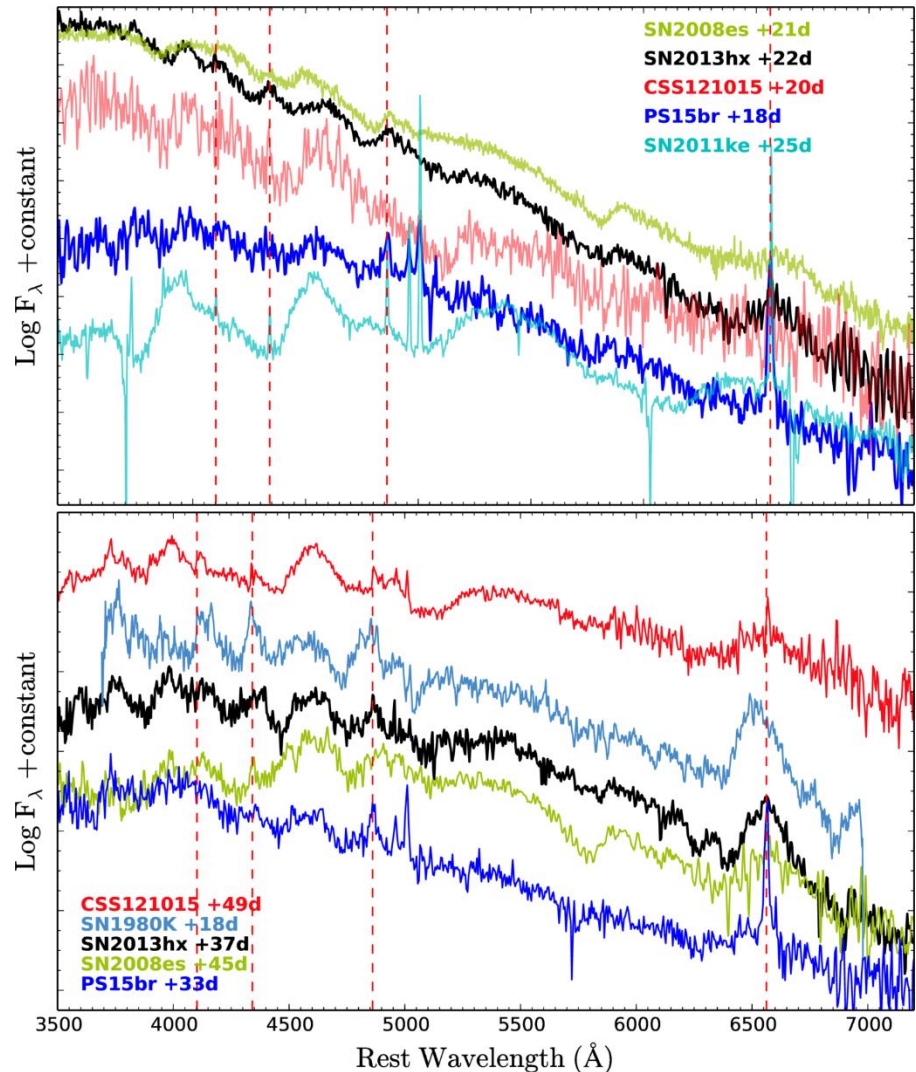
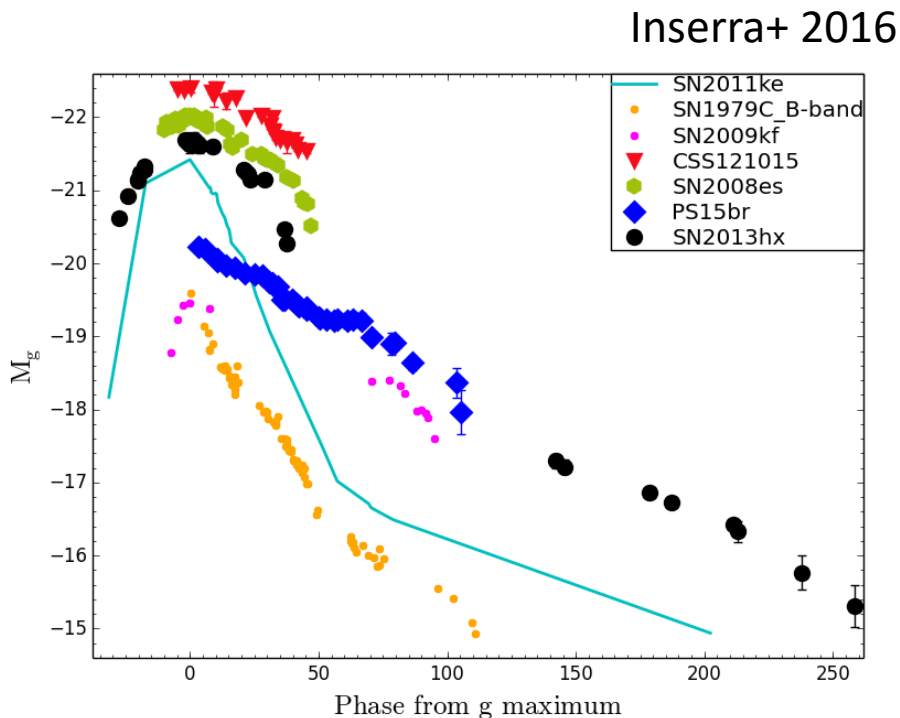
## SN Ia-CSM (SN 2012ca)

II n lines overlying Ia spectrum  
e.g. Dilday+2012, Silverman+2013

**(Perley 2014)**

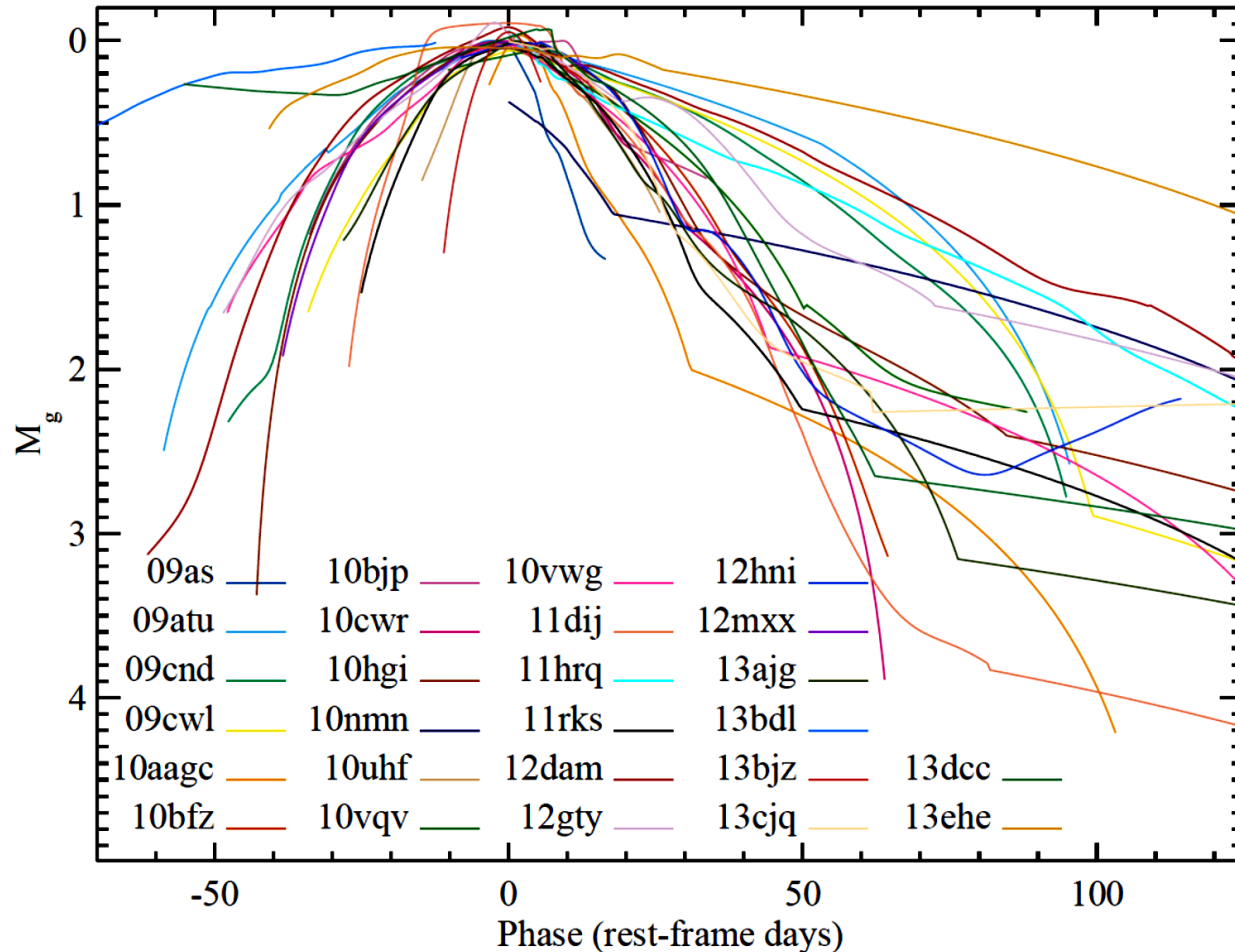
# Hydrogen-rich (**Type II**) SLSNe

- Type IIn (SN 2006gy) are attributed to CSM interaction (narrow and intermediate width hydrogen emission lines)
- The hot blue continuum and high peak luminosity happened early, late interaction for some SLSN-II



# Hydrogen-poor(**Type I**) PTF SLSN light curves

- Smoothed light curves of 26 PTF SLSNe normalized at peak (**De Cia+2017**)

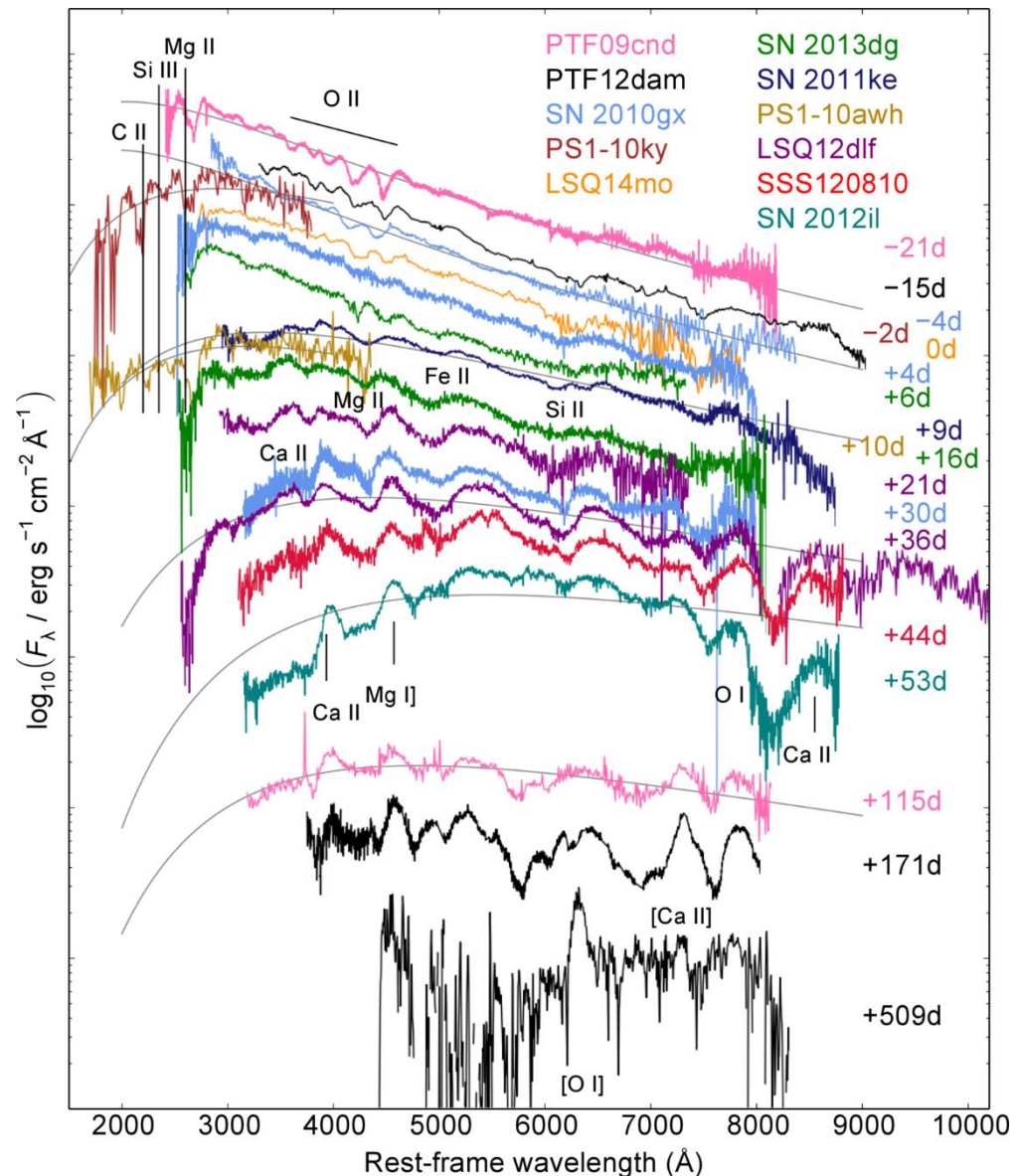


- No obvious gap between rapidly- and slowly-declining events

# PTF SLSN-I spectroscopy

(Nicholl+ 2015)

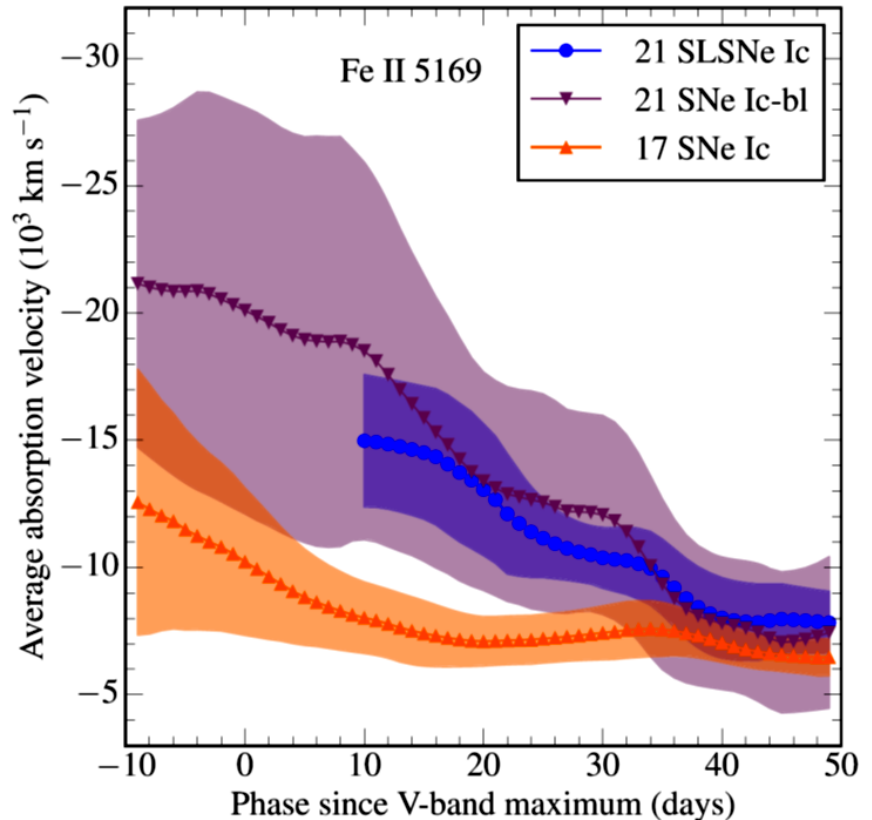
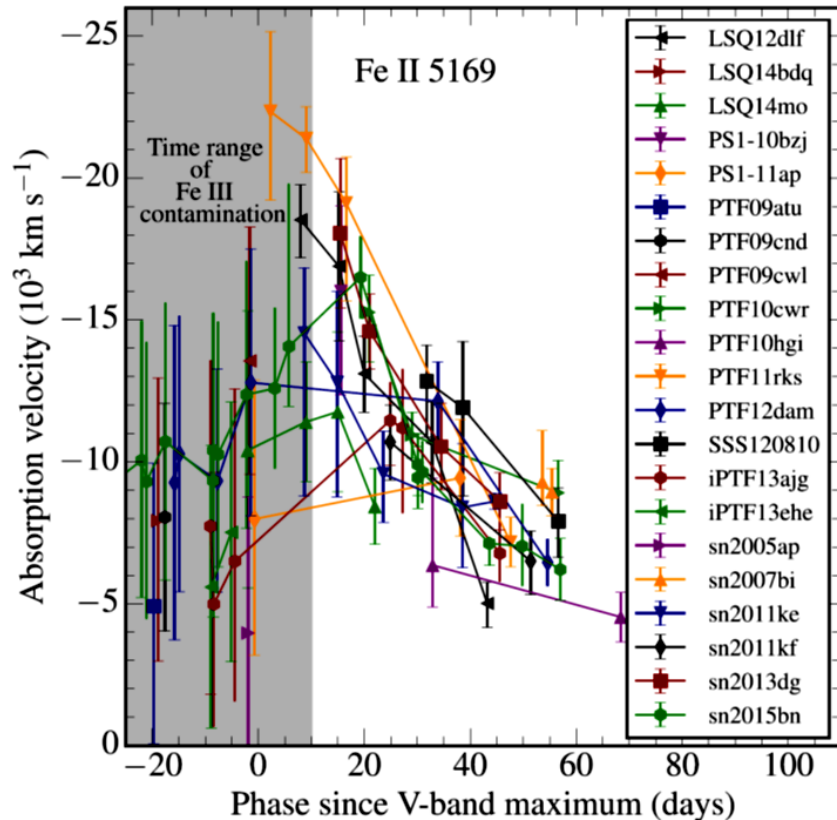
- Series of 5 lines of O II, which may persist until shortly after maximum light (signature of the class?).
- After oxygen recombination (around 15,000 K) maximum Ca II H&K, Mg II, Si II, and Fe II. A few weeks after maximum, SLSNe-I start to resemble SNe Ic at maximum light
- Velocities are comparable to normal Ic:  
10500±3100km/s for SLSNe,  
9800±2500km/s for Ic,  
slower decline for SLSNe



# Fe II $\lambda 5169\text{\AA}$ absorption velocities

(Liu+ 2017)

- No systematic difference in velocities for SLSNe Ic between fast-declining light curves and slow-declining light curves.
- Similarities in observations indicate that SLSNe Ic and SNe Ic-bl may have similar explosion engines, which is consistent with a multi-D magnetar model in Suzuki & Maeda (2017).



# SLSN Host Galaxies

(Perley 2017)

- **High metallicity strongly suppresses SLSNe-I**

Low ( $< 1/2$  Solar), but not *very* low

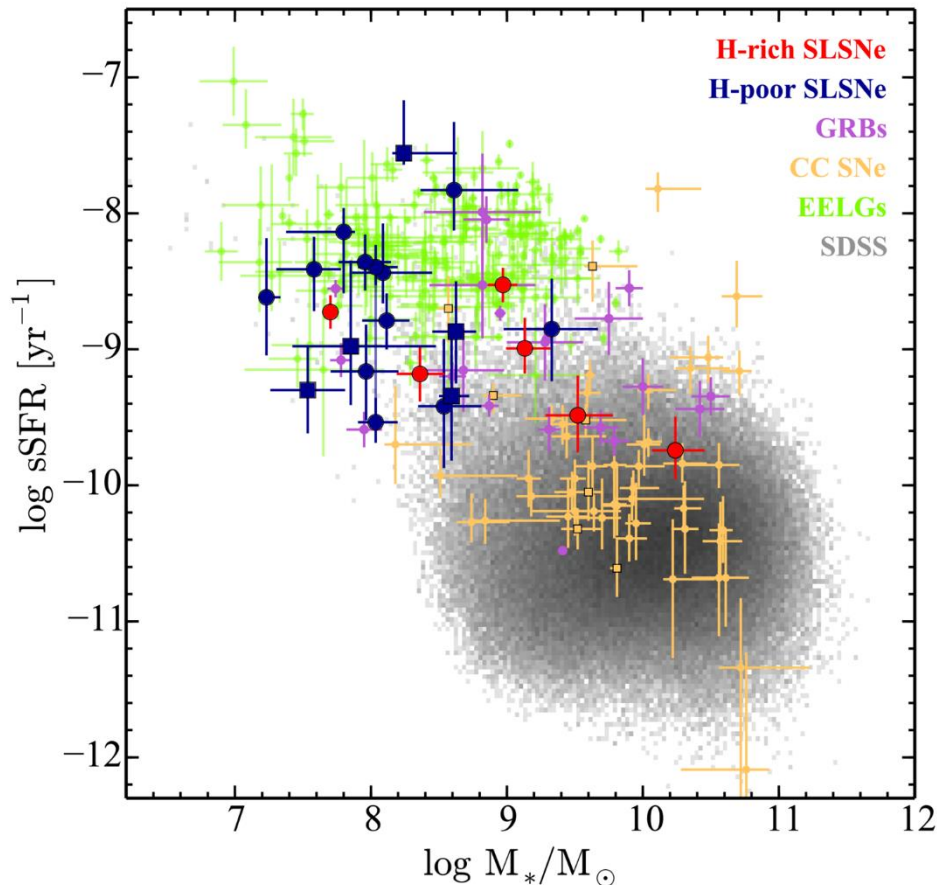
(Leloudas+2005)

- **The approximate cosmic rate is low, but significant**

$\sim 1/3000$  supernovae at  $z \sim 0$ , on average. But,  $\sim 1/600$  in metal-poor galaxies.

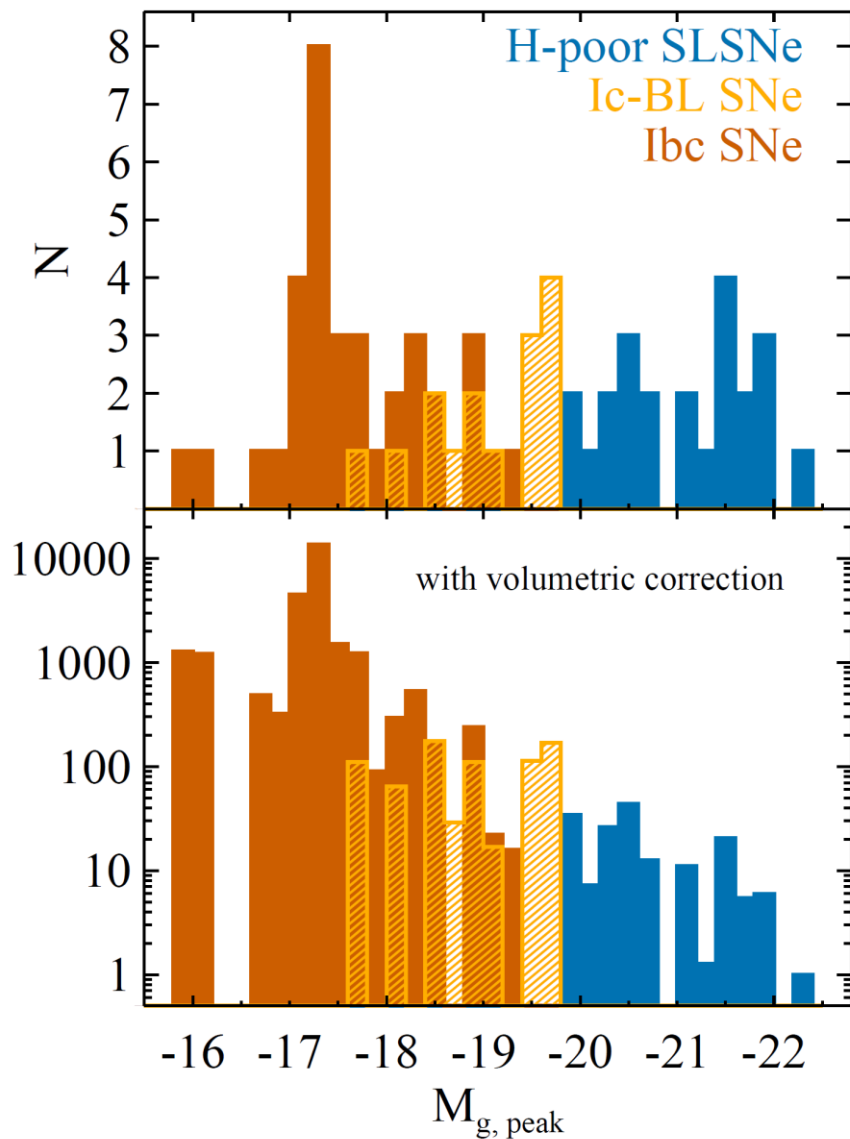
- **SLSNe-I have distinct environments from other SNe**  
SLSNe-I, SLSN-II, GRBs, and (other) cc-SNe all have statistically different host populations

- **SLSNe-I may prefer the most intensely star-forming galaxies**  
Partially (entirely?) a side-effect of metallicity preference.

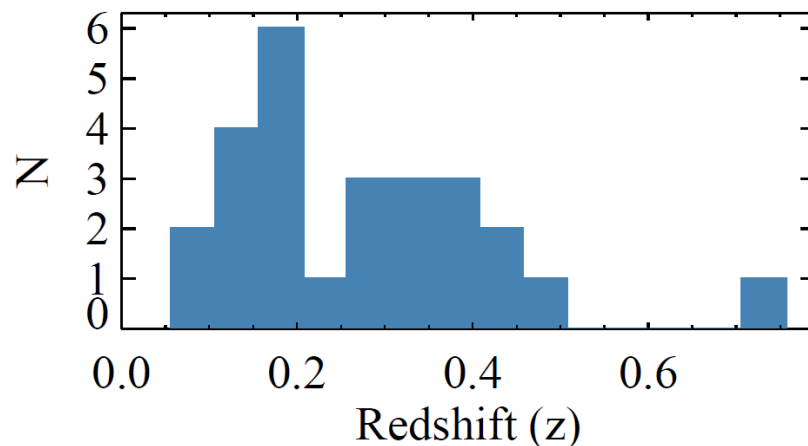


# Peak – magnitude and redshift distributions (PTF)

(De Cia+ 2017)

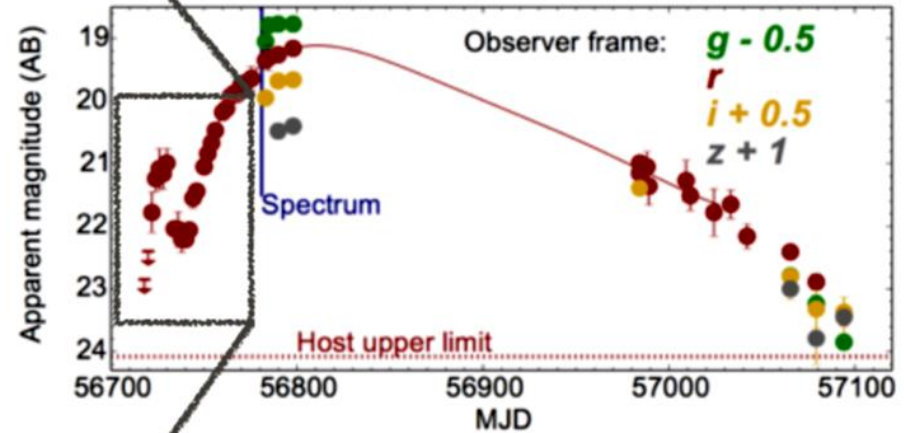
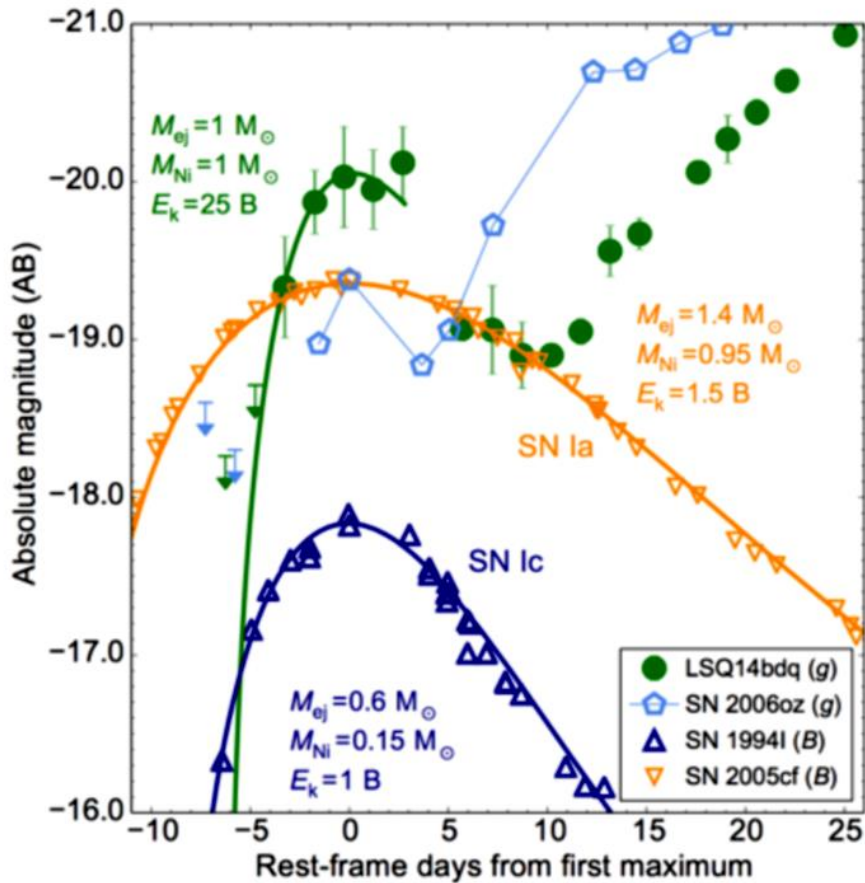


- Higher redshift (up to  $z \sim 4$ ). JWST is expected to be able to detect SLSNe out to  $z \sim 20$  (Abbott+ 2017).
- PTF typically discovers SLSNe below  $z < 1$ .
- Pan-STARRS1 SLSNe tend to be at higher redshift ( $z > 0.5$ ).



# Doubled peak of SLSN-I (by R. Quimby)

Similar to SN 1994I (Type Ic) but is much brighter, much narrower than the SN Ia 2005cf.



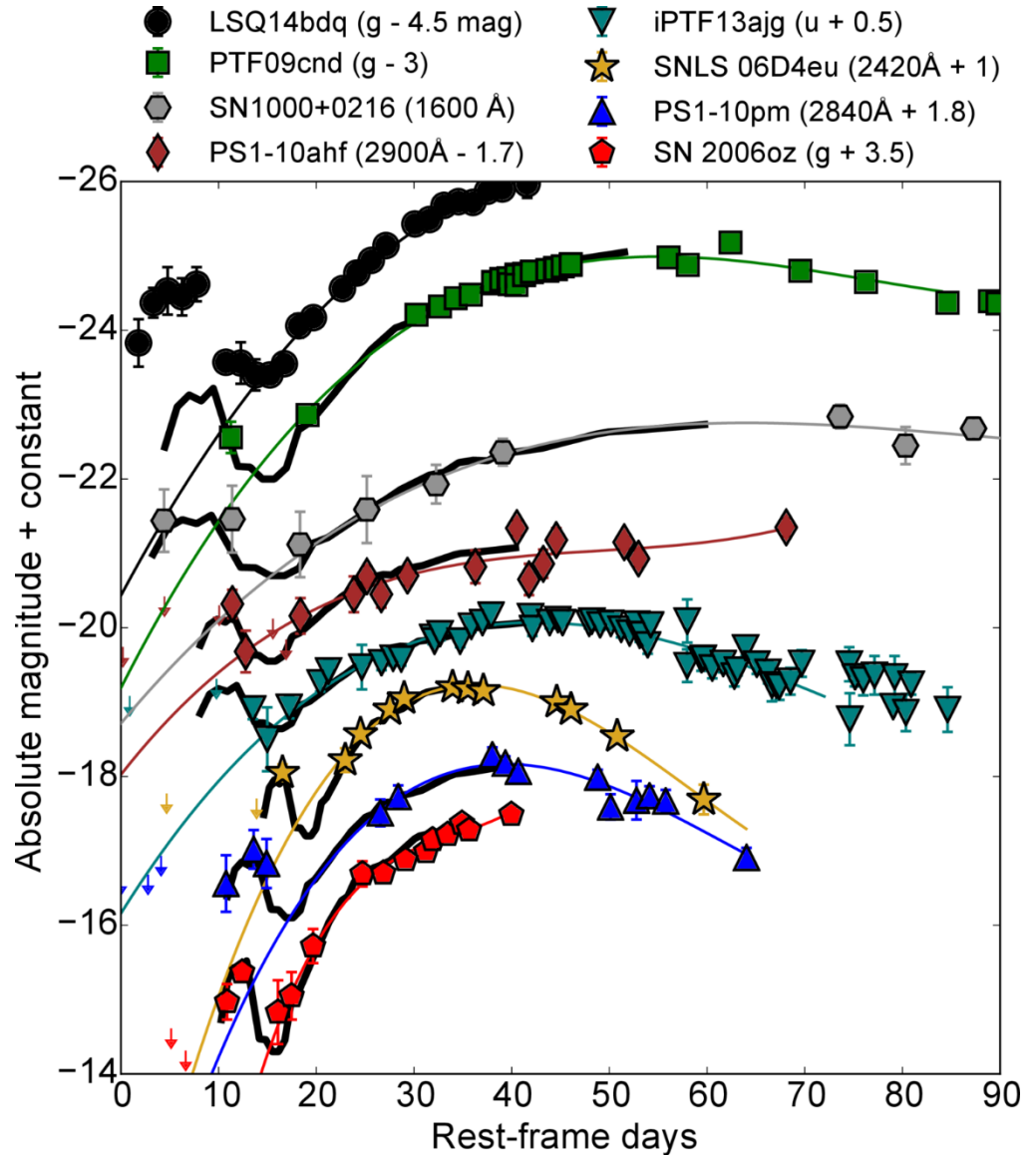
Nicholl et al. (2015)

See also Leloudas et al. 2012  
Nicholl & Smartt 2016  
Kasen et al. 2016

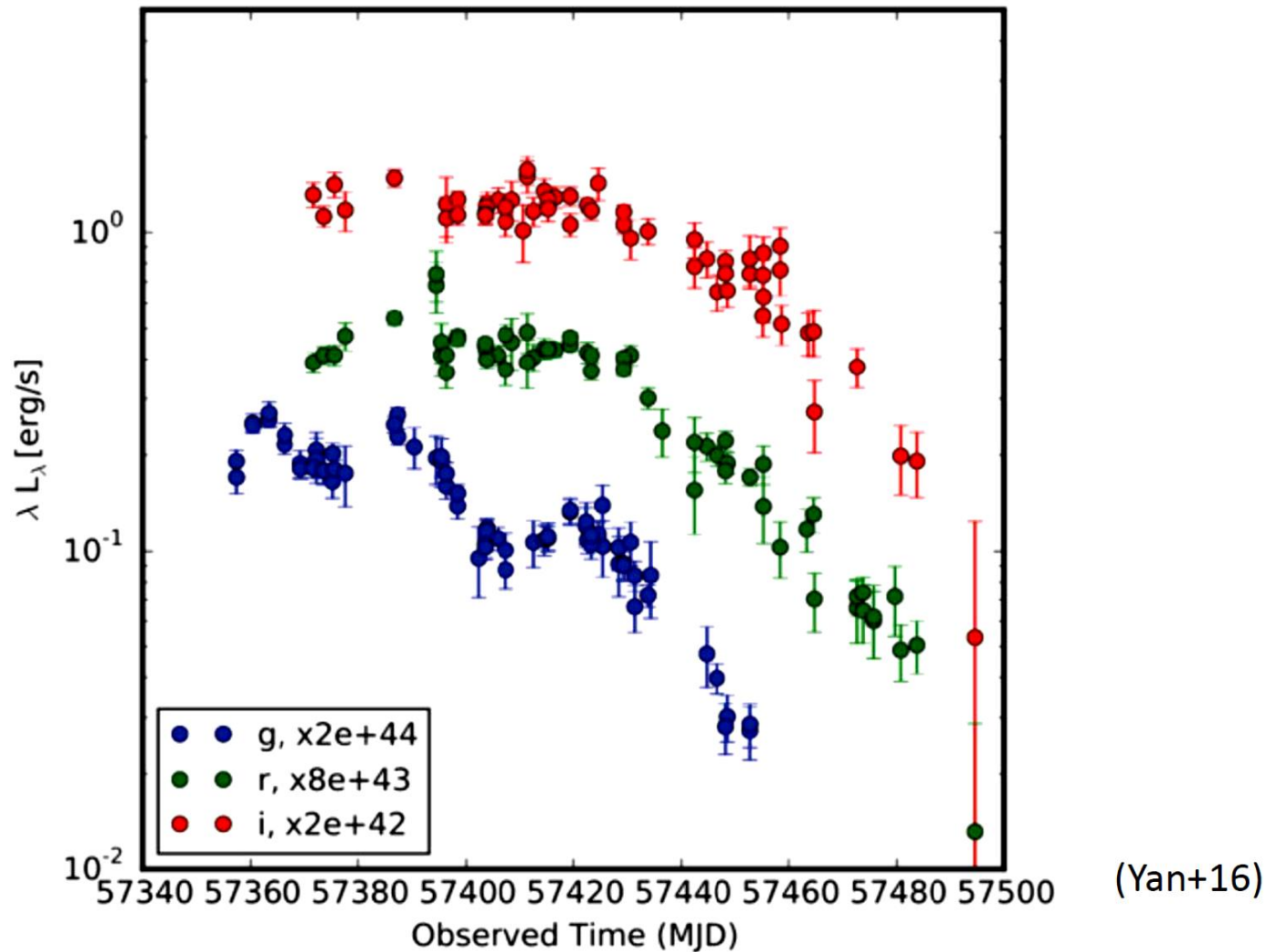
# Doubled peak of SLSN-I

(Nicholl+2016)

- 8 of 14 SLSN-I with early data
- Shock breakout
- Postshock cooling
- Interaction with CSM
- $T \sim 20,000$  K and rapid cooling, consistent with a shock in extended materia (Smith+2016)

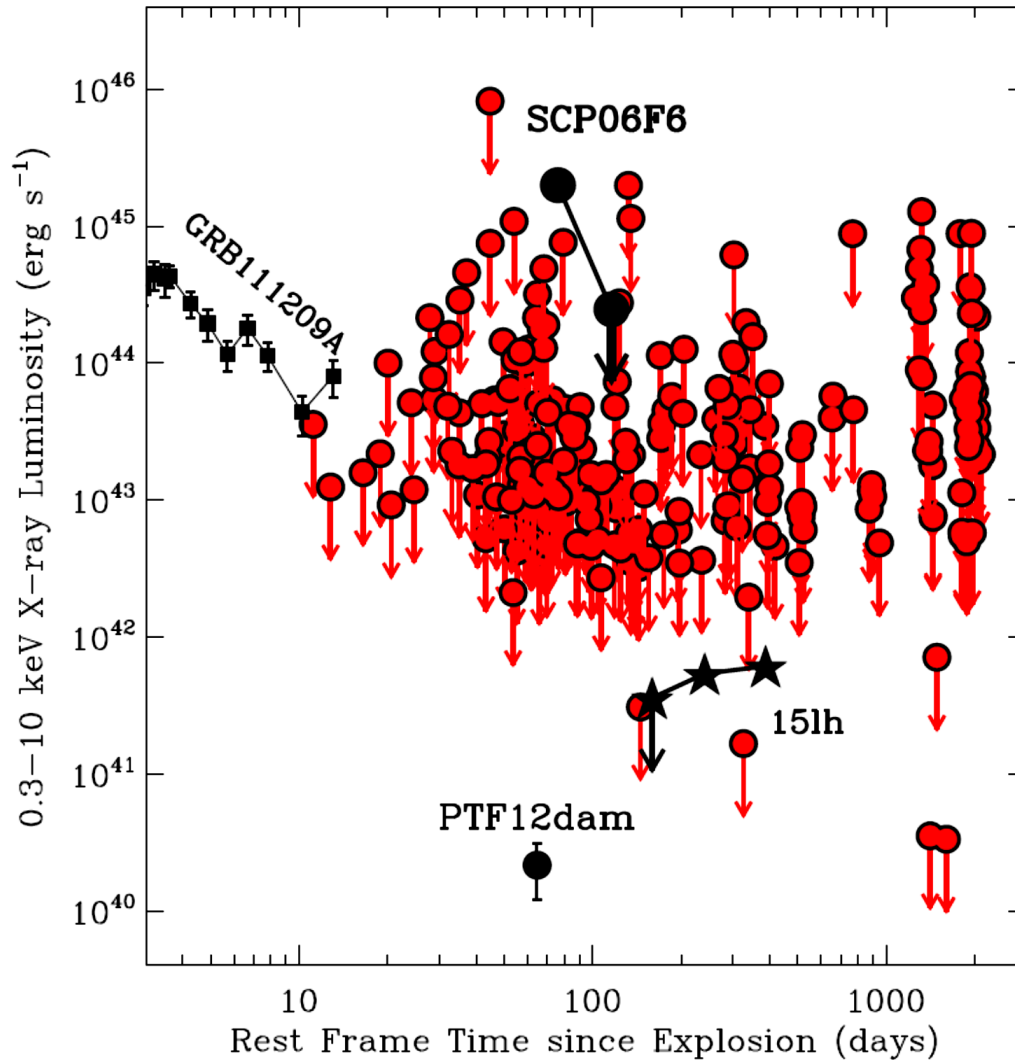


# SLSN-I PTF15esb: bumpy light curve



- Multiple-shell CSM interaction model. Late-time H (+100d). He?

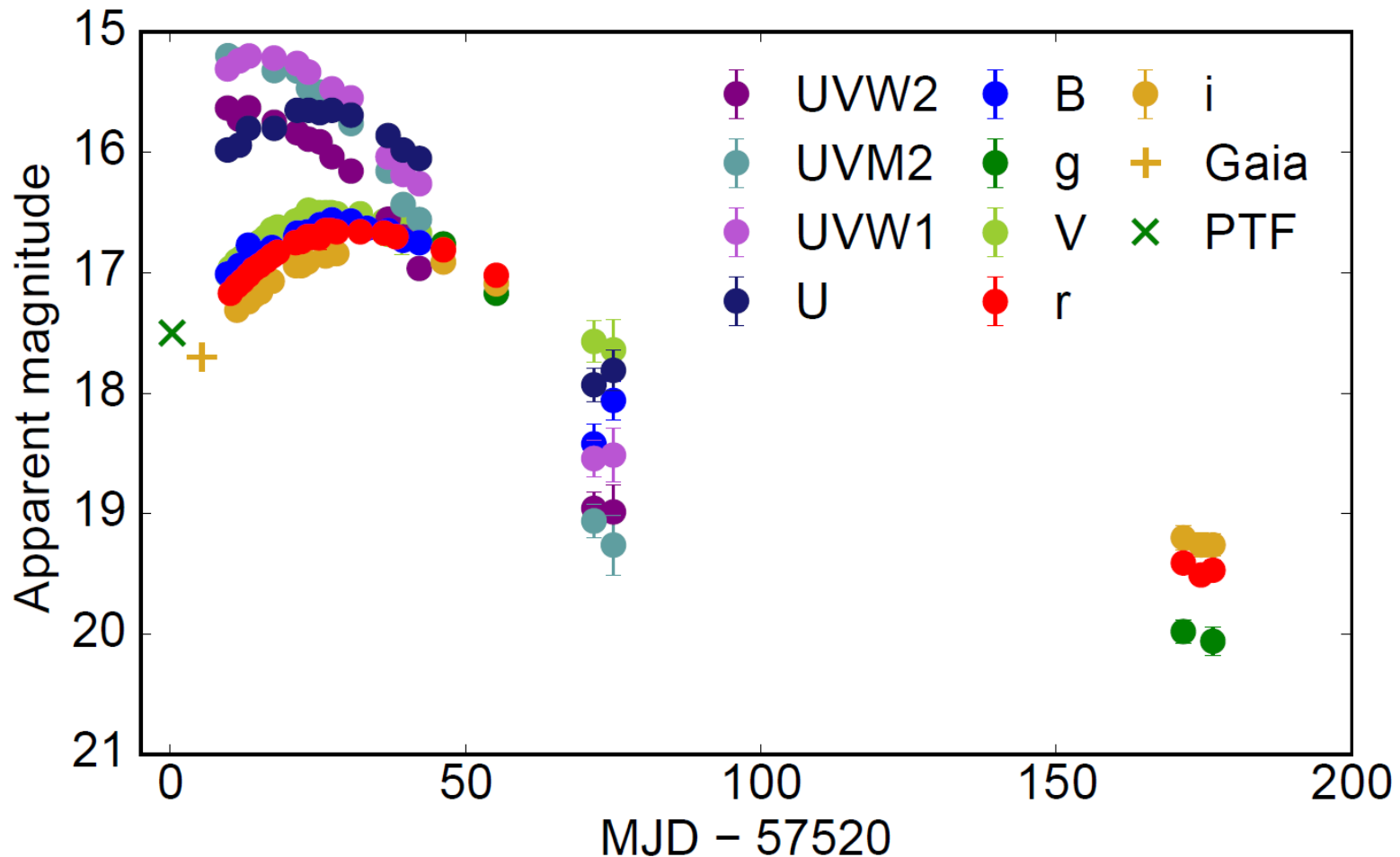
# X-ray observations of SLSN-I



- 26 nearby SLSN-I with Swift, Chandra and XMM (Margutti 2017)
- X-ray observations of SLSNe-I spanning the time range 10–2000 days (red circles for upper limits, black circles for detections) show that superluminous X-ray emission of the kind detected at the location of SCP06F6

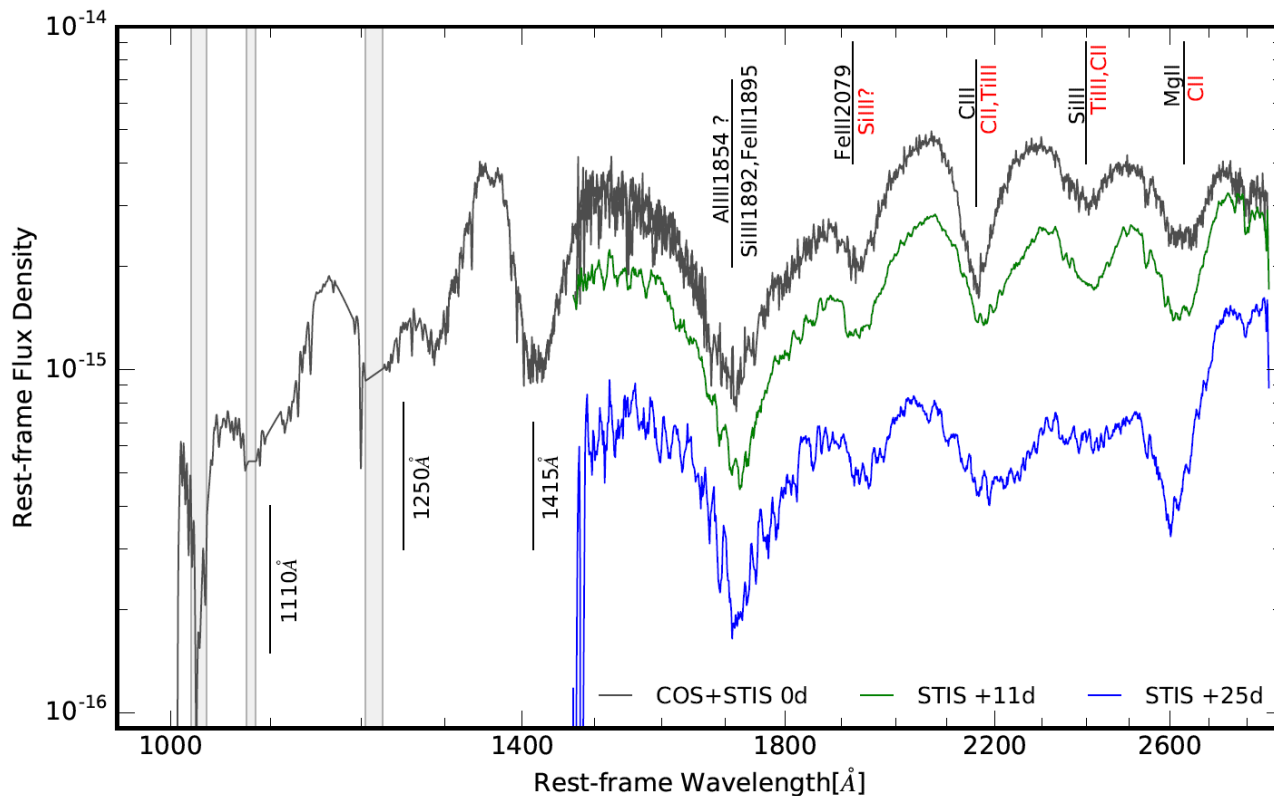
# Hydrogen-poor UV-bright Gaia16apd

- Extraordinarily UV-bright emission among superluminous supernovae (Kangas et al. 2017; Yan et al. 2017; Nicholl 2017)



# Gaia16apd far-UV spectrum (Yan+17)

- The complete and reliable identification of the UV absorption features requires future detailed modeling
- Tentative comparison with the published synthetic UV spectra (made available by D. Kasen) suggests that Gaia16apd may be an explosion of a massive C+O core with a sub-solar metal abundance



# SLSN-I Gaia16apd (SN 2016eay)

- (Yan+17)  $z=0.1018$ ,  $L=3 \cdot 10^{44}$  erg,  $t_{\text{rise}}=33\text{d}$  (uncertain up to 72d), 50% luminosity in 1000-2500Å. Spectrum is similar to PS1-11bam, 6 spectral features similar to SN1992A, SN2017fe (SNIa), ejecta velocity 14,000 km/s, no X-rays
- (Kangas+17), spectroscopically similar to PTF12dam,  $v=15,600 \dots 19,800$  km/s from -16.2d to +2.8d; 12,700-12,400 from +2.8d to +43d;  $v=10,000$  at +150d
- Interaction?                      Magnetar?                      PISN?

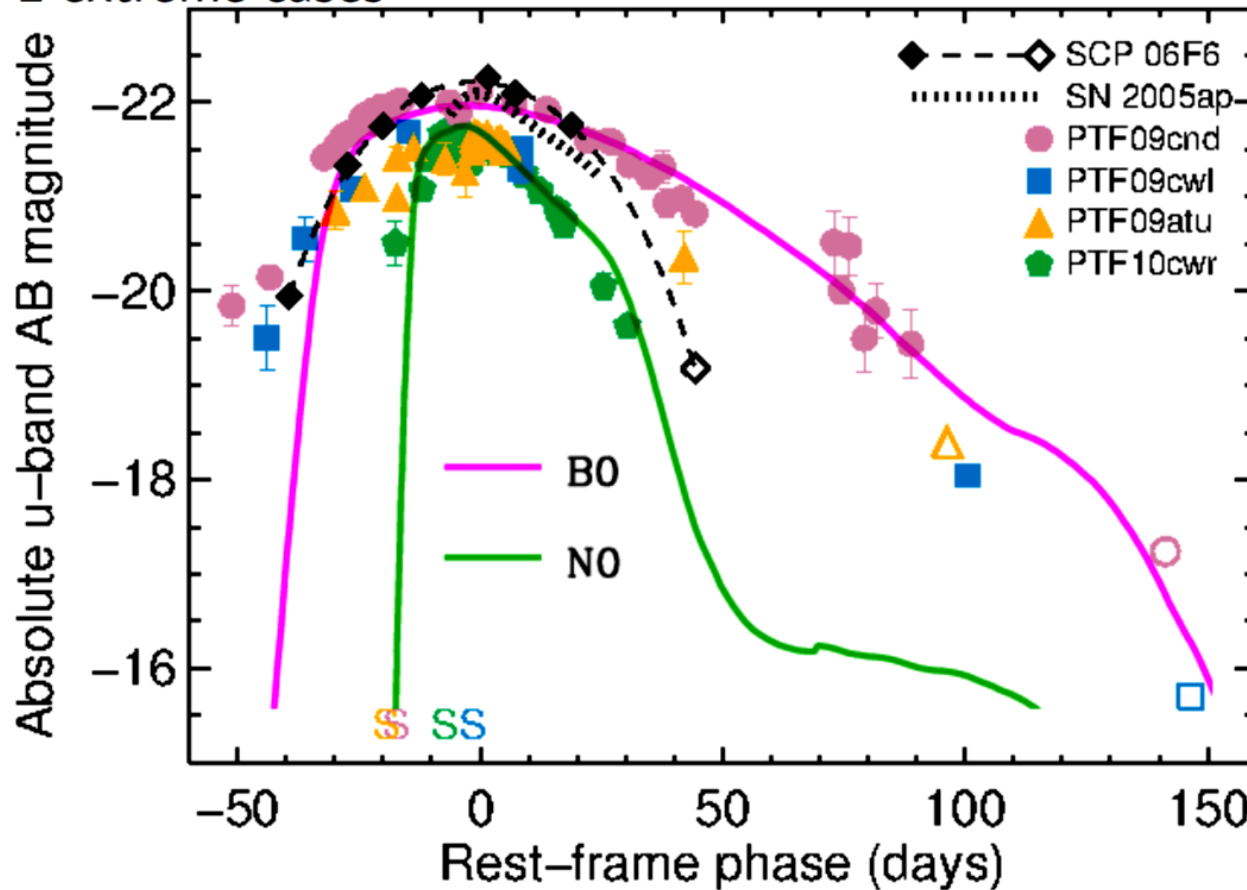


(Image credit: Kavli IPMU)

# Arguments for interaction model

(Sorokina+ 2016)

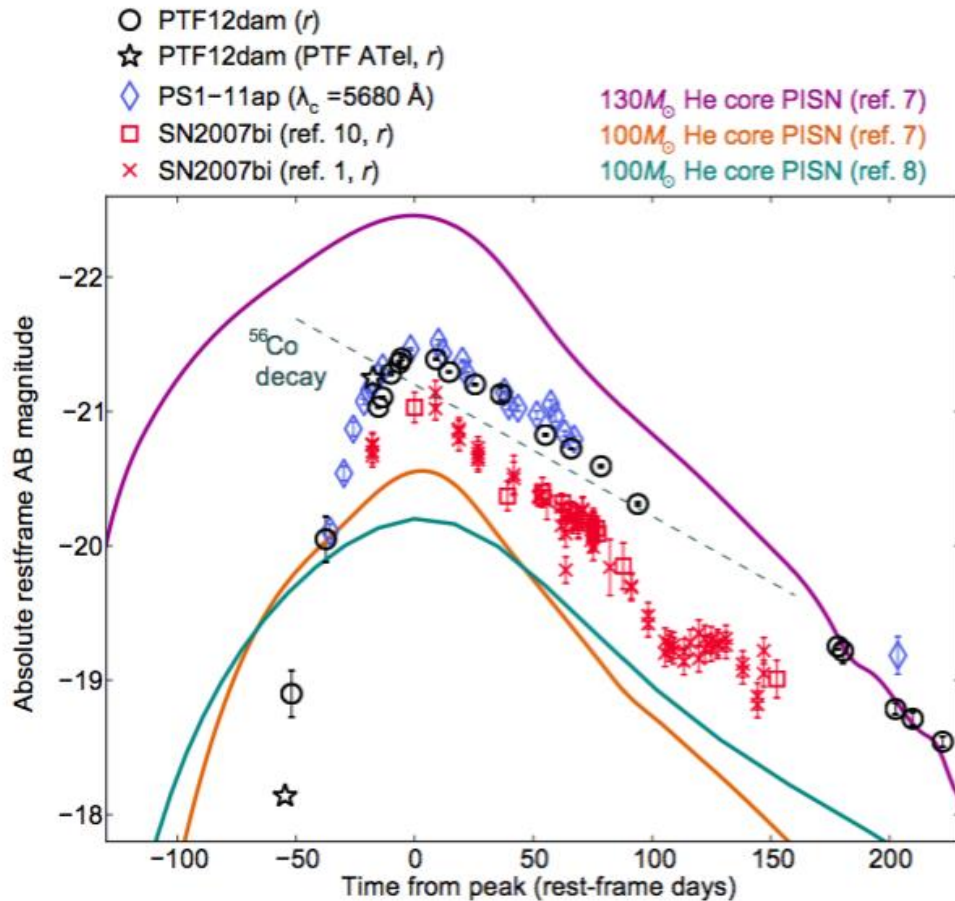
- STELLA reproduces a wide range of SLSNe in the interaction model:  
2 extreme cases



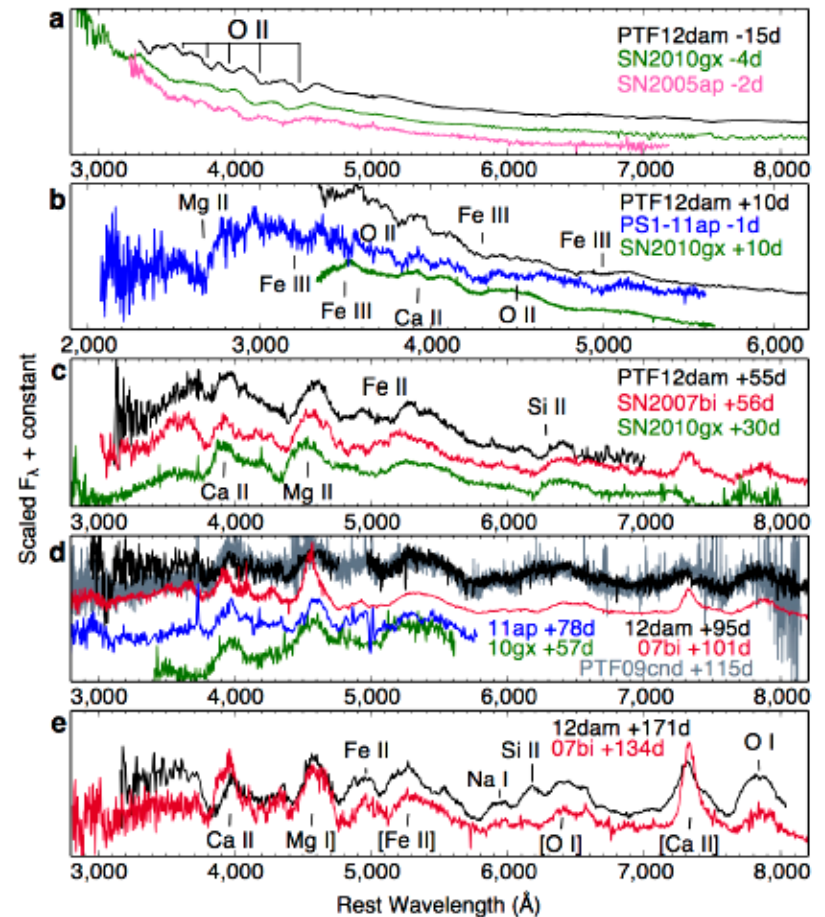
Explosion energy is just 2 - 4 foe

# SLSN I-R PTF12dam: light curves and spectra

- Optical light curves of slow-fading SLSN (Nicholl et al. 2013)

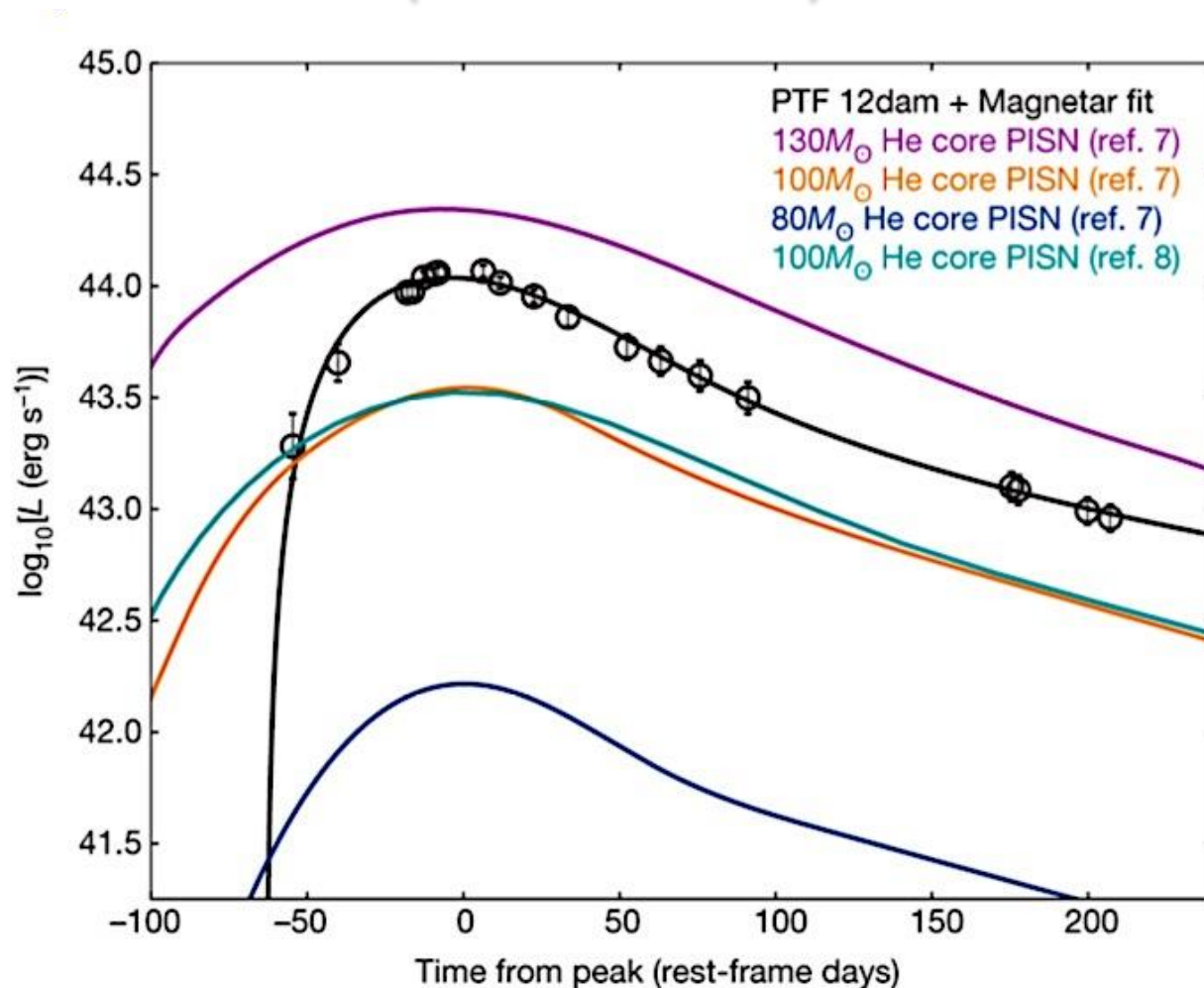


- Spectral evolution of PTF12dam (Nicholl et al. 2013), lack of hydrogen/helium



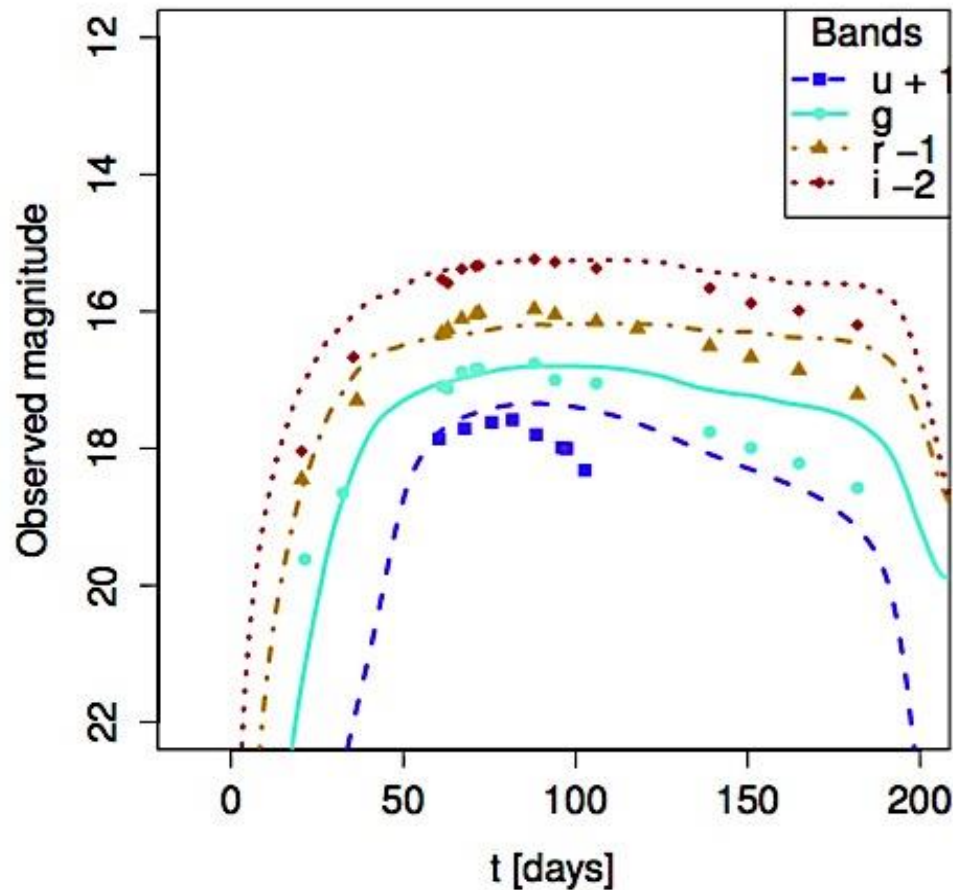
# PTF12dam: bolometric light curves and “magnetar” fit

(Nicholl et al. 2013)



- “Magnetar” fits are based on oversimplified models.
- The spin-down energy is converted into shell kinetic energy – **Not into luminosity!** (Badjin, Barkov, Blinnikov, in prep)

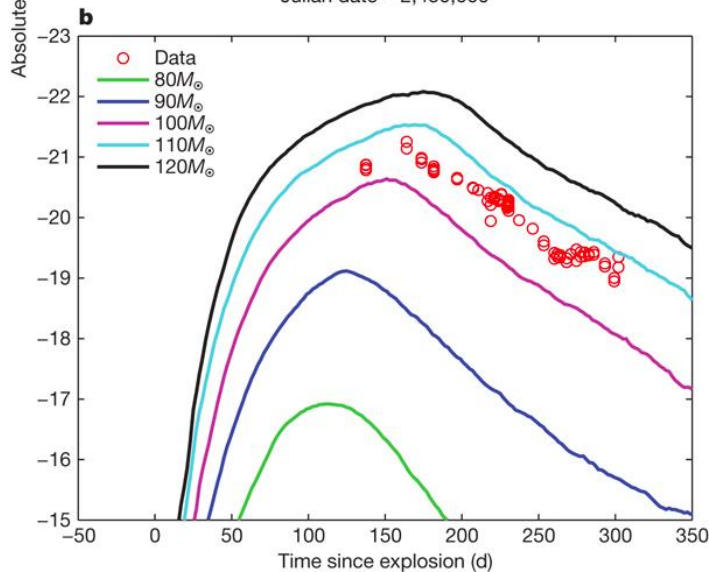
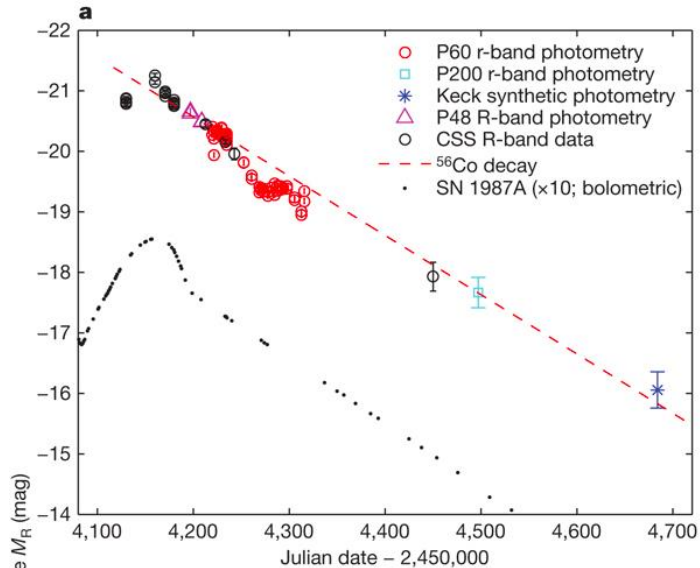
# Simulated and observed light curves (Baklanov et al. 2015)



Ejecta  $5 M_{\odot}$ , “wind”  $48 M_{\odot}$  of He, explosion 4 foe. Perhaps not He, but C/O, and larger mass may be needed for long “tail”. Here radioactive heating may help.

# SN 2007bi: PISN, CCSN models

- Gal-Yam et al. 2009



- Moriya et al. 2010

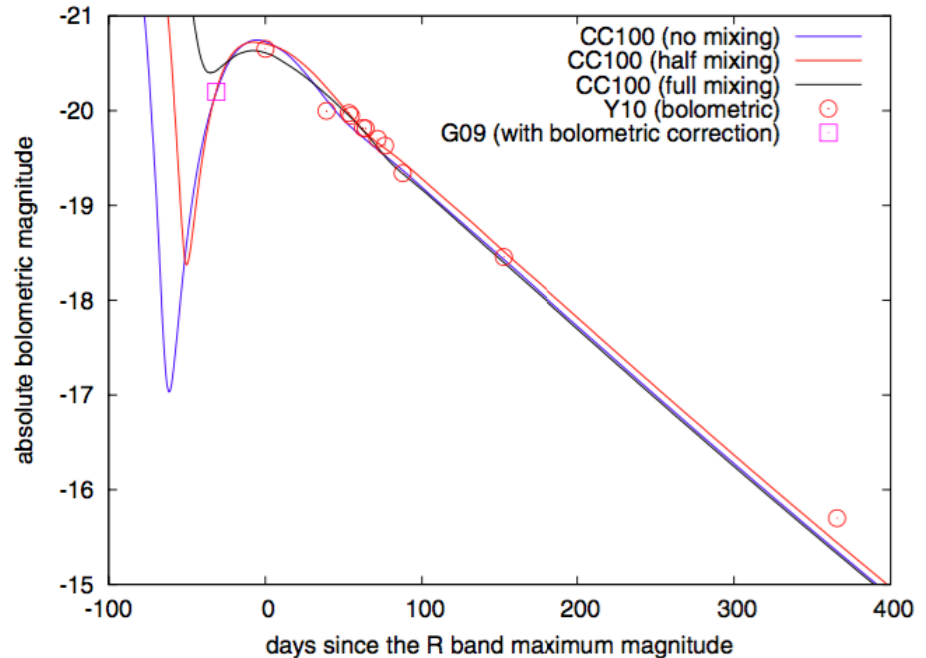
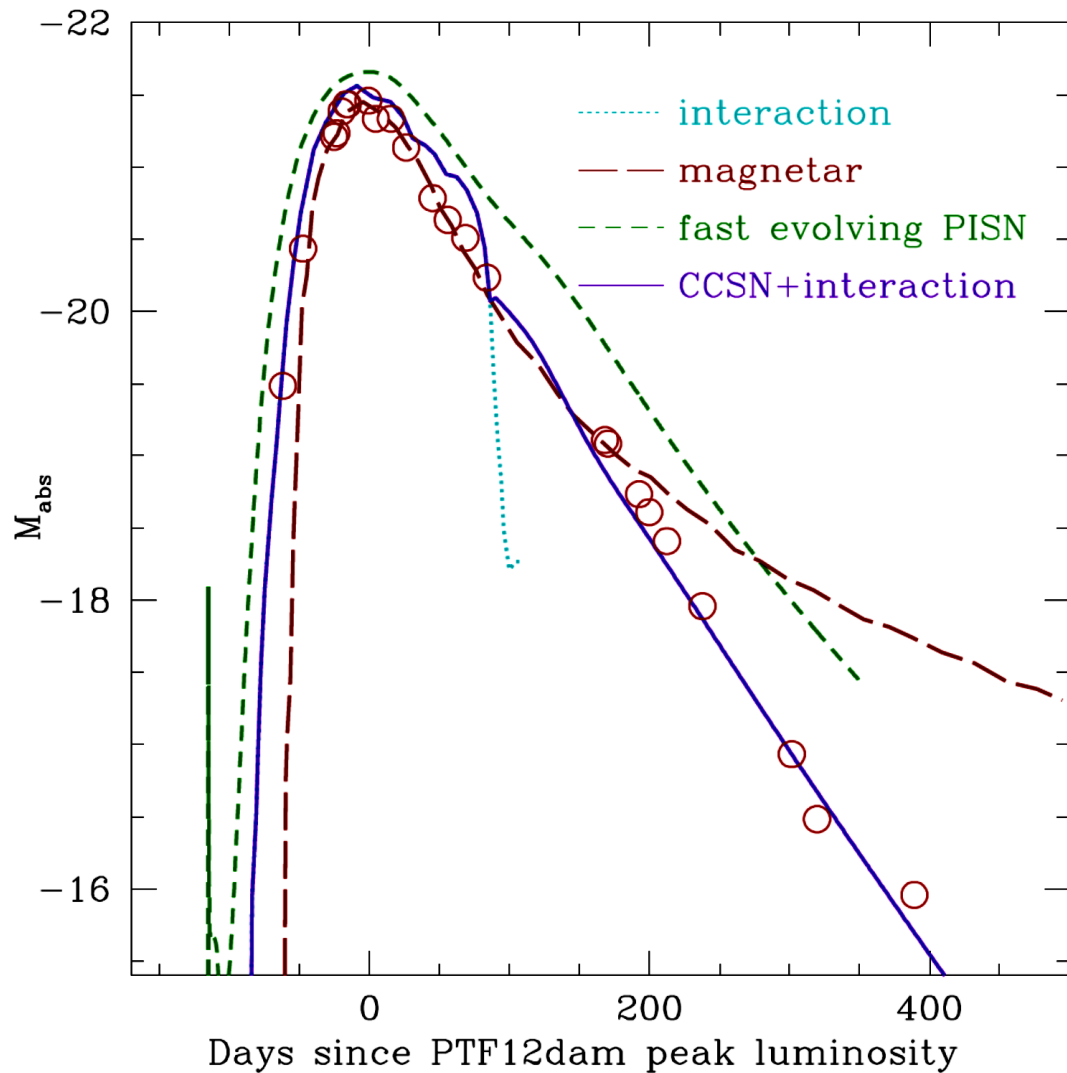


**Figure 1.** Bolometric LCs of the C+O star SN models CC100 ( $M_{\text{ej}} = 40 M_{\odot}$ ,  $E_{\text{kin}} = 3.6 \times 10^{52}$  erg, and  $M_{56\text{Ni}} = 6.1 M_{\odot}$ ). The observed bolometric LC (open circles) is taken from Y10. The bolometric magnitude of the rising part of SN 2007bi (open square) is estimated from the R-band magnitude. All the calculated LCs have the same physical structure but the degrees of mixing are different. The horizontal axis shows the days in the rest frame.

**Figure 2:** Radioactive  $^{56}\text{Ni}$  and total ejected mass from the light-curve evolution of SN 2007bi are well fitted using PISN models.

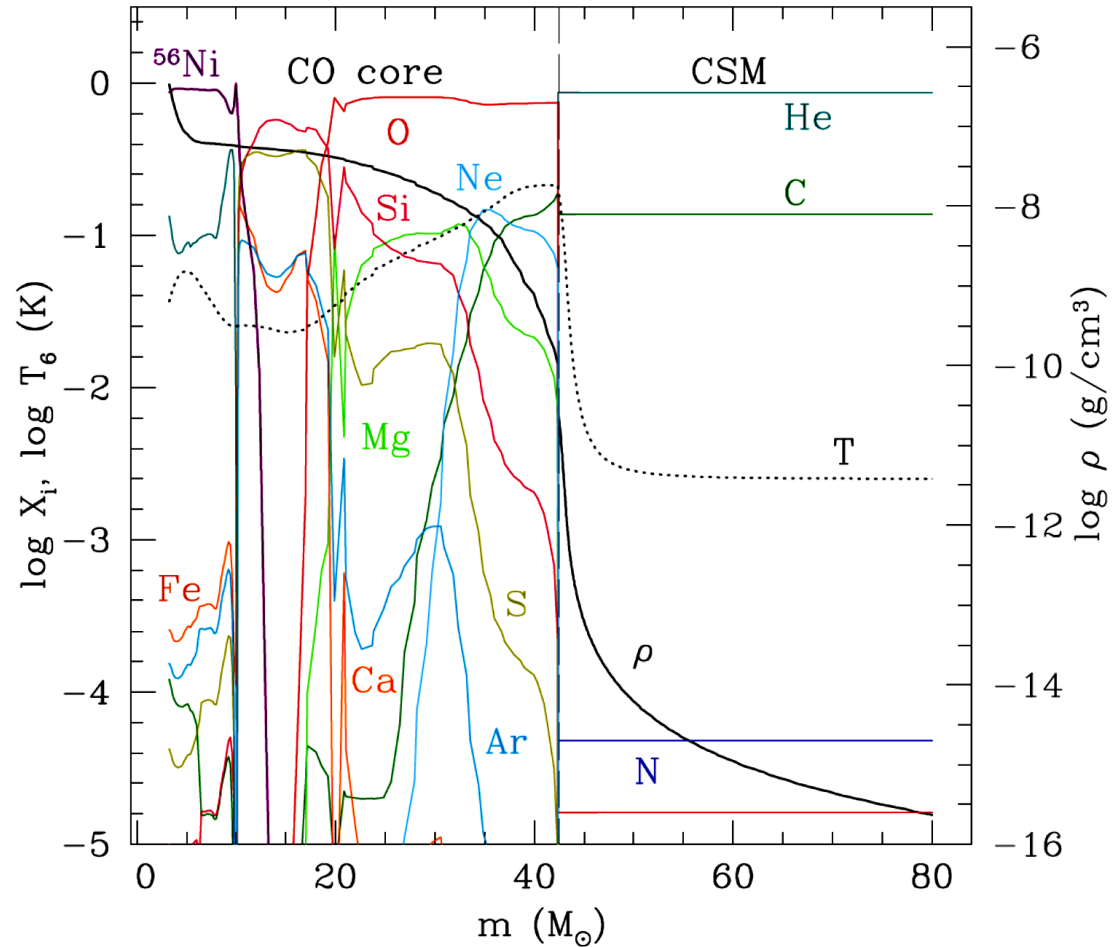
# PTF12dam: PISN, CCSN models



- Bolometric light curves of PTF12dam in observations and models (Chen 2014, Nicholl et al 2013, Kozyreva 2017, Baklanov et al 2015)

# Interaction model: composition and structure of pre-SN

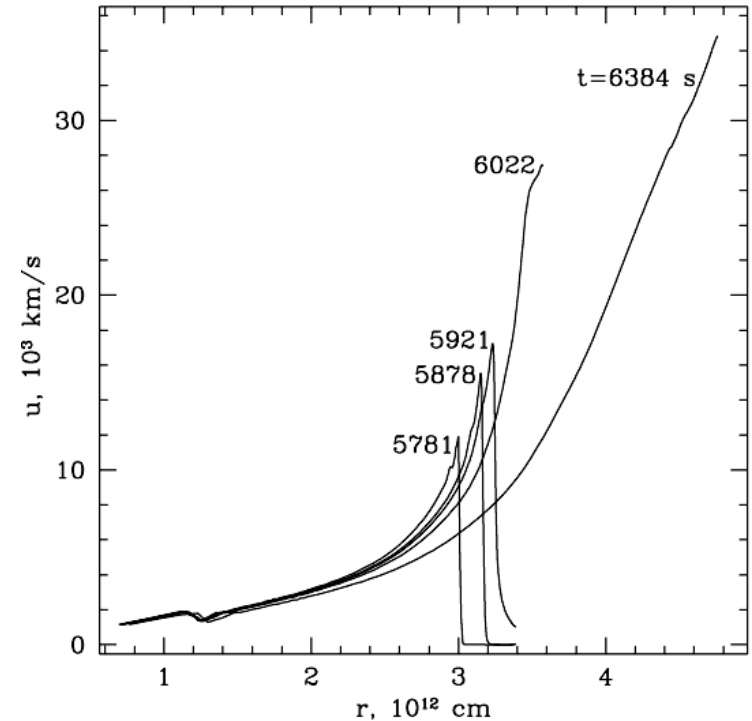
- $M_{\text{ZAMS}} = 100 M_{\odot}$ ,  $Z = Z_{\odot} / 200$  (Umeda&Nomoto 2008)
- PTF12dam: pre-SN C+O core ( $43M_{\odot}$ ),  $M_{\text{cut}} = 3M_{\odot}$
- Postprocess explosive nucleosynthesis (used by Moriya et al. (2010) for SN 2007bi)
- 1 day hydro after explosion + extended CSM
- Parameters:  $M_{\text{CSM}}$ ,  $R_{\text{CSM}}$ ,  $T_{\text{CSM}}$ ,  $M(^{56}\text{Ni})$ , composition of CSM



# Numerical code STELLA

## **STELLA** (Static Eddington-factor Low-velocity Limit Approximation) (Blinnikov et al. 1998)

- 1D Lagrangian Hydro + Radiation Moments Equations (2D), VEF closure, multigroup (100-300 groups, up to 1000  $\rightarrow$  rough SED), implicit scheme. Shock is initiated by thermal bomb.
- Opacity includes photoionization, free-free absorption, lines and electron scattering (Blandford & Payne 1981). Ionization – Saha's approximation.
- STELLA was used in modeling of many SN light curves: SN 1987A, SN 1993J and many others (Blinnikov et al. 2006). Models with CSM, magnetar, PISNe.
- STELLA-lite version is integrated in MESA (Paxton+2017)



- Matter velocity at the epoch of shock breakout versus Eulerian radius  $r$  (bottom) in the model for SN 1987A from Blinnikov (1999). The proper time is given near the curves.

# Comoving radiative transfer equation (Mihalas 1980)

Transfer equation:

$$\begin{aligned}
 & \frac{\gamma}{c} (1 + \beta\mu_0) \frac{\partial I_0(\mu_0, \nu_0)}{\partial t} + \gamma(\mu_0 + \beta) \frac{\partial I_0(\mu_0, \nu_0)}{\partial r} \\
 & + \gamma(1 - \mu_0^2) \left[ \frac{(1 + \beta\mu_0)}{r} - \frac{\gamma^2}{c} (1 + \beta\mu_0) \frac{\partial \beta}{\partial t} - \gamma^2(\mu_0 + \beta) \frac{\partial \beta}{\partial r} \right] \frac{\partial I_0(\mu_0, \nu_0)}{\partial \mu_0} \\
 & - \gamma \left[ \frac{\beta(1 - \mu_0^2)}{r} + \frac{\gamma^2}{c} \mu_0(1 + \beta\mu_0) \frac{\partial \beta}{\partial t} + \gamma^2 \mu_0(\mu_0 + \beta) \frac{\partial \beta}{\partial r} \right] \nu_0 \frac{\partial I_0(\mu_0, \nu_0)}{\partial \nu_0} \\
 & + 3\gamma \left[ \frac{\beta(1 - \mu_0^2)}{r} + \frac{\gamma^2 \mu_0}{c} (1 + \beta\mu_0) \frac{\partial \beta}{\partial t} + \gamma^2 \mu_0(\mu_0 + \beta) \frac{\partial \beta}{\partial r} \right] I_0(\mu_0, \nu_0) \\
 & = \eta_0(\nu_0) - \chi_0(\nu_0) I_0(\mu_0, \nu_0).
 \end{aligned}$$

Moment equations:

$$\begin{aligned}
 & \frac{\gamma}{c} \left[ \frac{\partial J_0(\nu_0)}{\partial t} + \beta \frac{\partial H_0(\nu_0)}{\partial t} \right] + \gamma \left[ \frac{\partial H_0(\nu_0)}{\partial r} + \beta \frac{\partial J_0(\nu_0)}{\partial r} \right] \\
 & - \gamma \nu_0 \left\{ \frac{\beta}{r} \left[ \frac{\partial J_0(\nu_0)}{\partial \nu_0} - \frac{\partial K_0(\nu_0)}{\partial \nu_0} \right] + \frac{\gamma^2}{c} \frac{\partial \beta}{\partial t} \left[ \frac{\partial H_0(\nu_0)}{\partial \nu_0} + \beta \frac{\partial K_0(\nu_0)}{\partial \nu_0} \right] + \gamma^2 \frac{\partial \beta}{\partial r} \left[ \frac{\partial K_0(\nu_0)}{\partial \nu_0} + \beta \frac{\partial H_0(\nu_0)}{\partial \nu_0} \right] \right\} \\
 & + \gamma \left\{ \frac{2}{r} [H_0(\nu_0) + \beta J_0(\nu_0)] + \frac{\gamma^2}{c} \frac{\partial \beta}{\partial t} [H_0(\nu_0) + \beta J_0(\nu_0)] + \gamma^2 \frac{\partial \beta}{\partial r} [J_0(\nu_0) + \beta H_0(\nu_0)] \right\} \\
 & = \eta_0(\nu_0) - \chi_0(\nu_0) J_0(\nu_0) \\
 & \frac{\gamma}{c} \left[ \frac{\partial H_0(\nu_0)}{\partial t} + \beta \frac{\partial K_0(\nu_0)}{\partial t} \right] + \gamma \left[ \frac{\partial K_0(\nu_0)}{\partial r} + \beta \frac{\partial H_0(\nu_0)}{\partial r} \right] \\
 & - \gamma \nu_0 \left\{ \frac{\beta}{r} \left[ \frac{\partial H_0(\nu_0)}{\partial \nu_0} - \frac{\partial N_0(\nu_0)}{\partial \nu_0} \right] + \frac{\gamma^2}{c} \frac{\partial \beta}{\partial t} \left[ \frac{\partial K_0(\nu_0)}{\partial \nu_0} + \beta \frac{\partial N_0(\nu_0)}{\partial \nu_0} \right] + \gamma^2 \frac{\partial \beta}{\partial r} \left[ \frac{\partial N_0(\nu_0)}{\partial \nu_0} + \beta \frac{\partial K_0(\nu_0)}{\partial \nu_0} \right] \right\} \\
 & + \gamma \left\{ \frac{1}{r} [3K_0(\nu_0) - J_0(\nu_0) + \beta H_0(\nu_0) + \beta N_0(\nu_0)] + \frac{\gamma^2}{c} \frac{\partial \beta}{\partial t} [J_0(\nu_0) + 2\beta H_0(\nu_0) - \beta N_0(\nu_0)] \right. \\
 & \left. + \gamma^2 \frac{\partial \beta}{\partial r} [2H_0(\nu_0) - N_0(\nu_0) + \beta J_0(\nu_0)] \right\} = -\chi_0(\nu_0) H_0(\nu_0)
 \end{aligned}$$

# STELLA RADA integration (Tolstov2010)

## STELLA

Hydro

Radiation Moments

Static Eddington factors

Fluxes in comoving frame

**Output:** Fluxes  $o(v/c)$  in observer frame

HD relativistic corrections  
(Misner & Sharp, 1969)

$V \rightarrow V/[1+(V/C)^2]^{1/2}$

Doppler effect

## RADA (relativistic, time-dependant)

Boltzmann transport equation

Time-dependent Eddington factors

Fluxes in comoving frame

**Output:** Fluxes in observer frame

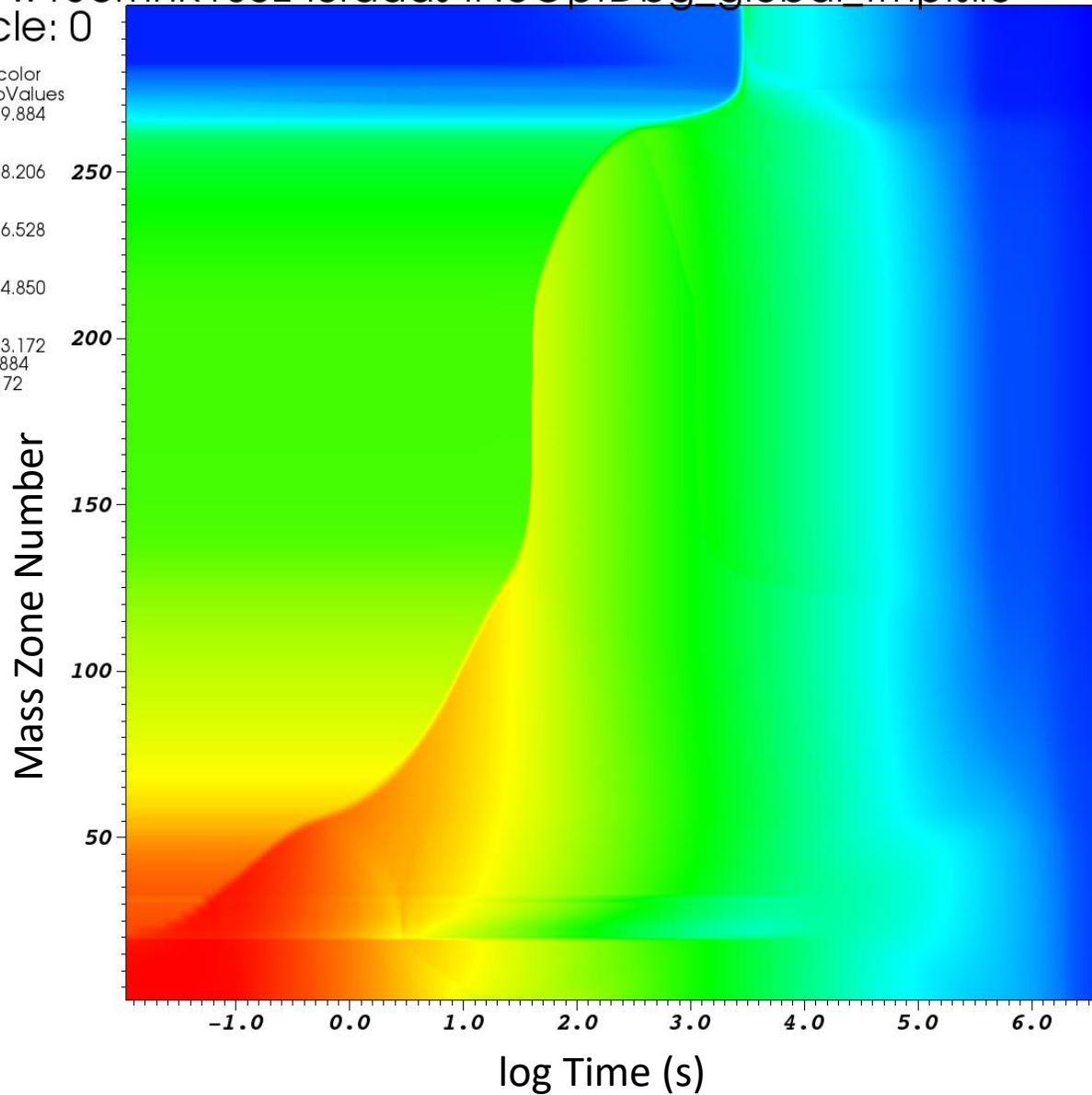
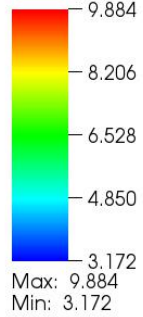


# Numerical code STELLA. Temperature diagram

DB: w13cmnR150E40radas4NoOptDbg\_global\_tmp.silo

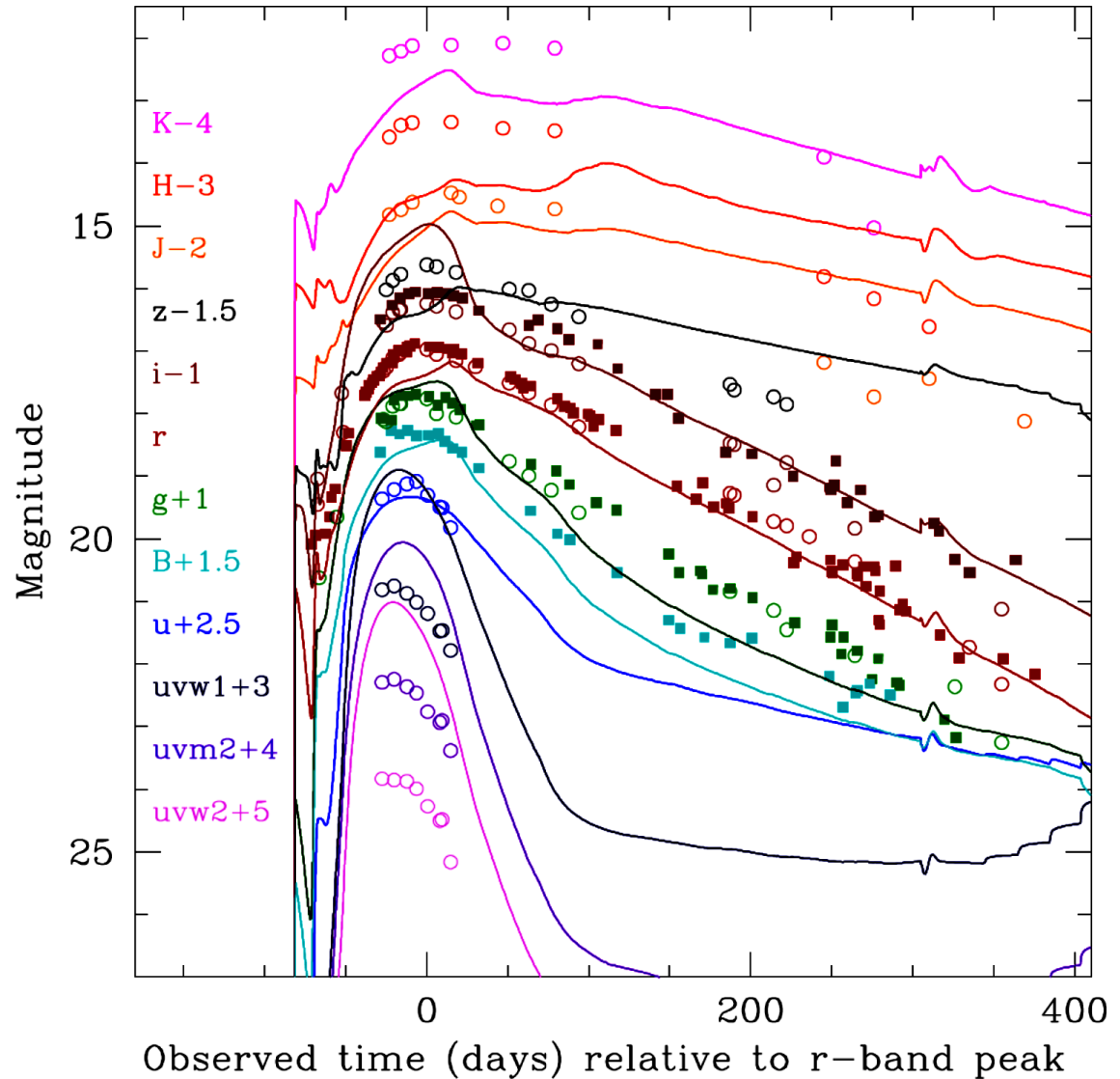
Cycle: 0

Pseudocolor  
Var: tmpValues



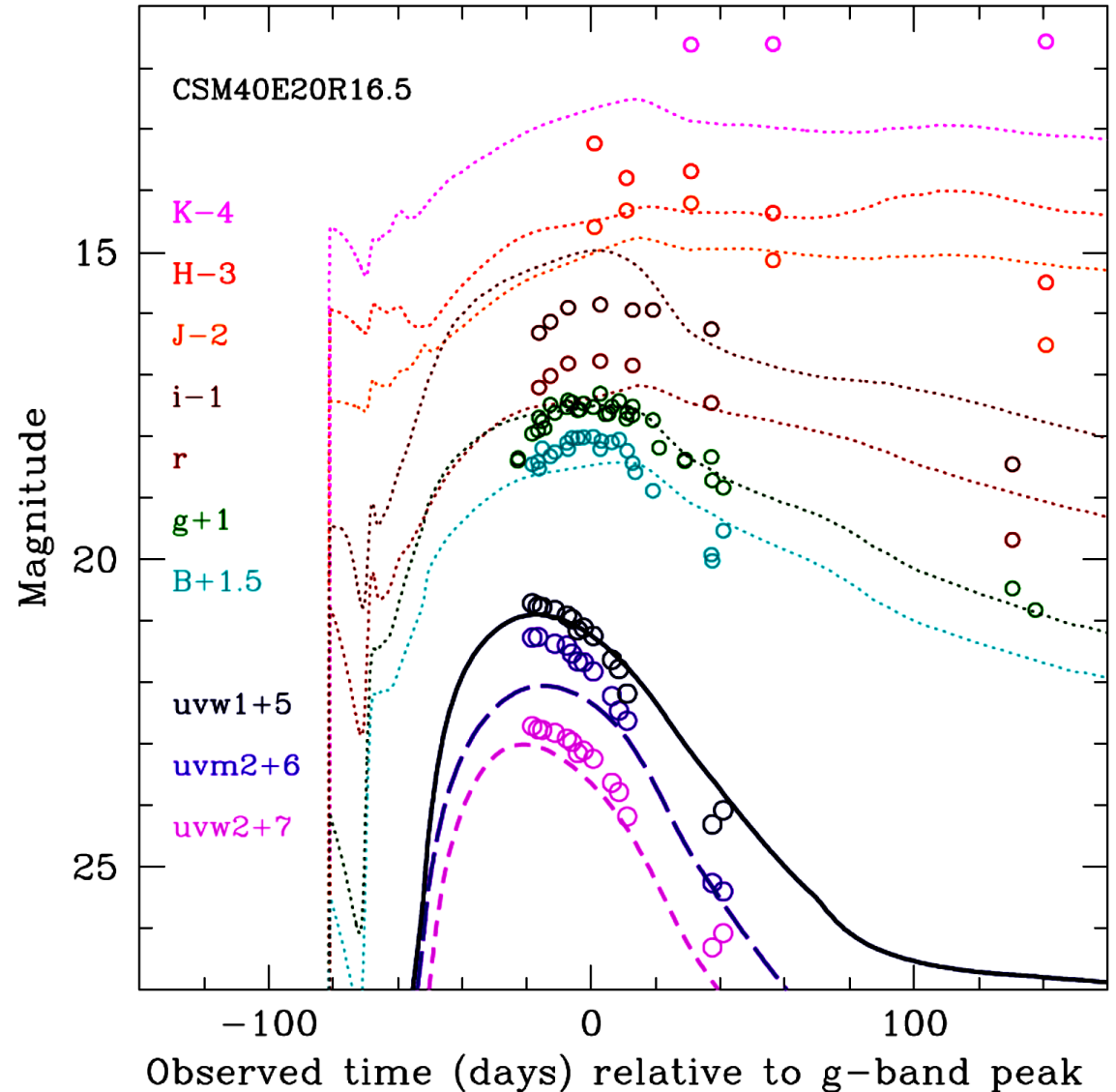
# PTF12dam R16 model. Multicolor light curves

Params	Value
$M_{\text{ej}}, M_{\odot}$	40
$M_{\text{CSM}}, M_{\odot}$	38
$T_{\text{CSM}}, \text{K}$	2500
$\lg R_{\text{CSM}}, \text{cm}$	16.5
$\rho$	2
$E_{51}$	20
$M(^{56}\text{Ni}), M_{\odot}$	6
AMHT, $M_{\odot}$	10
$X_{\text{CSM}}$	He:C=9:1



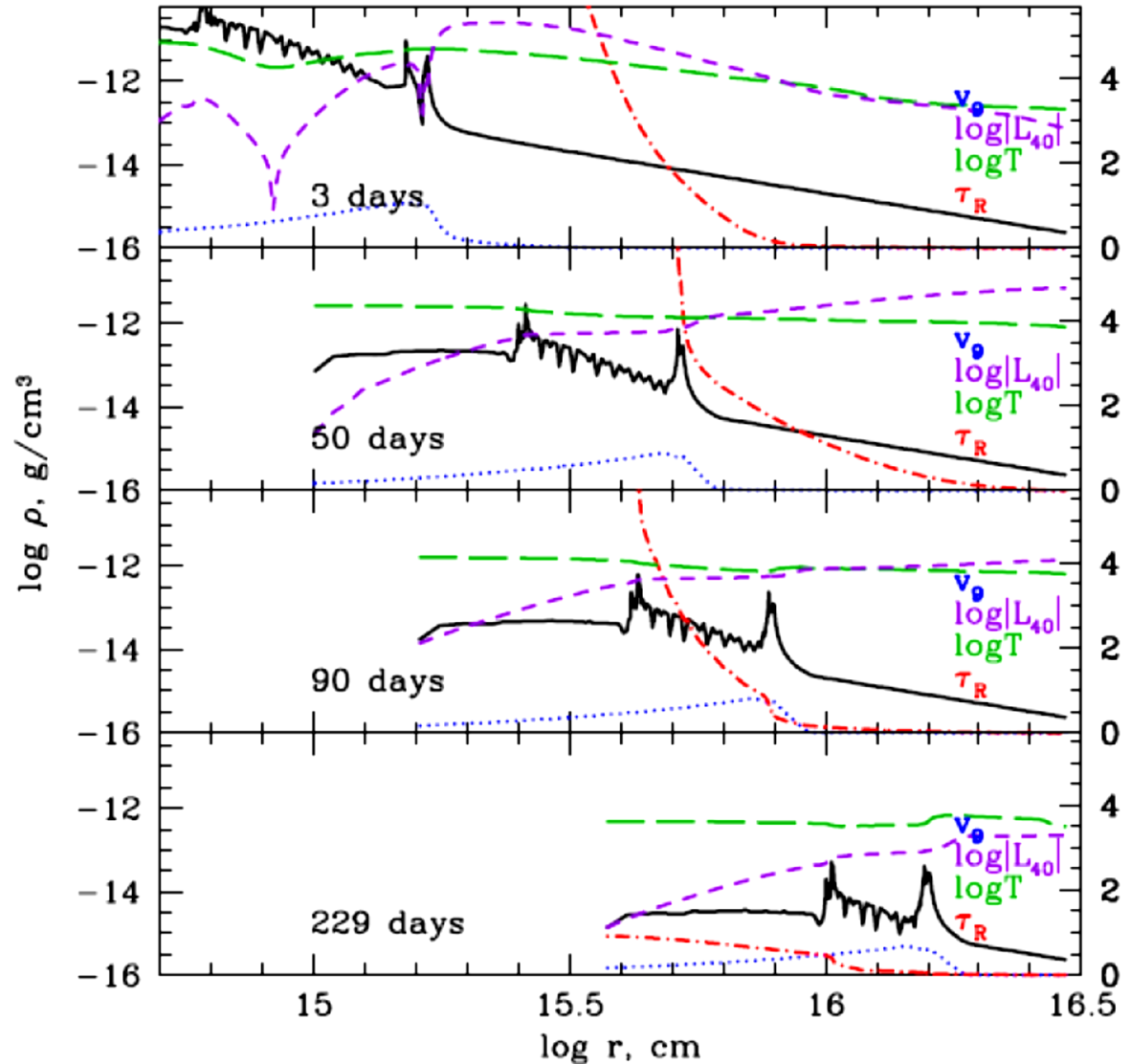
# Gaia16apd R16 model. Multicolor light curves

Params	Value
$M_{\text{ej}}, M_{\odot}$	40
$M_{\text{CSM}}, M_{\odot}$	38
$T_{\text{CSM}}, \text{K}$	2500
$\lg R_{\text{CSM}}, \text{cm}$	16.5
$\rho$	2
$E_{51}$	20
$M(^{56}\text{Ni}), M_{\odot}$	6
AMHT, $M_{\odot}$	10
$X_{\text{CSM}}$	He:C=9:1

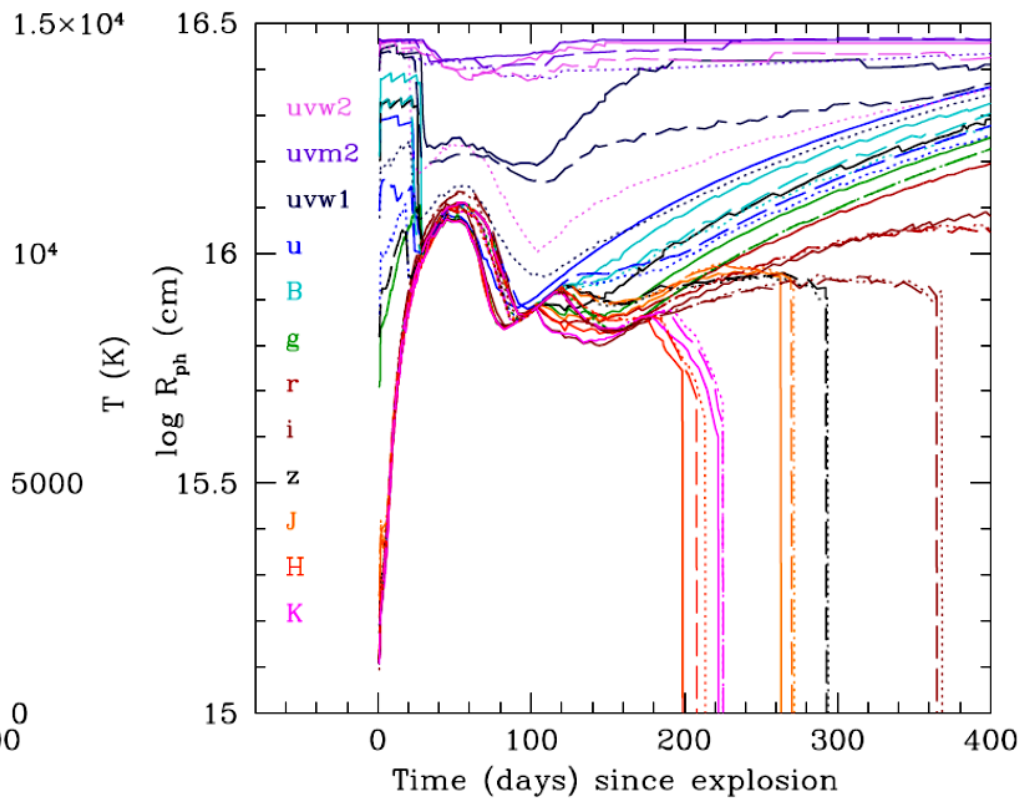
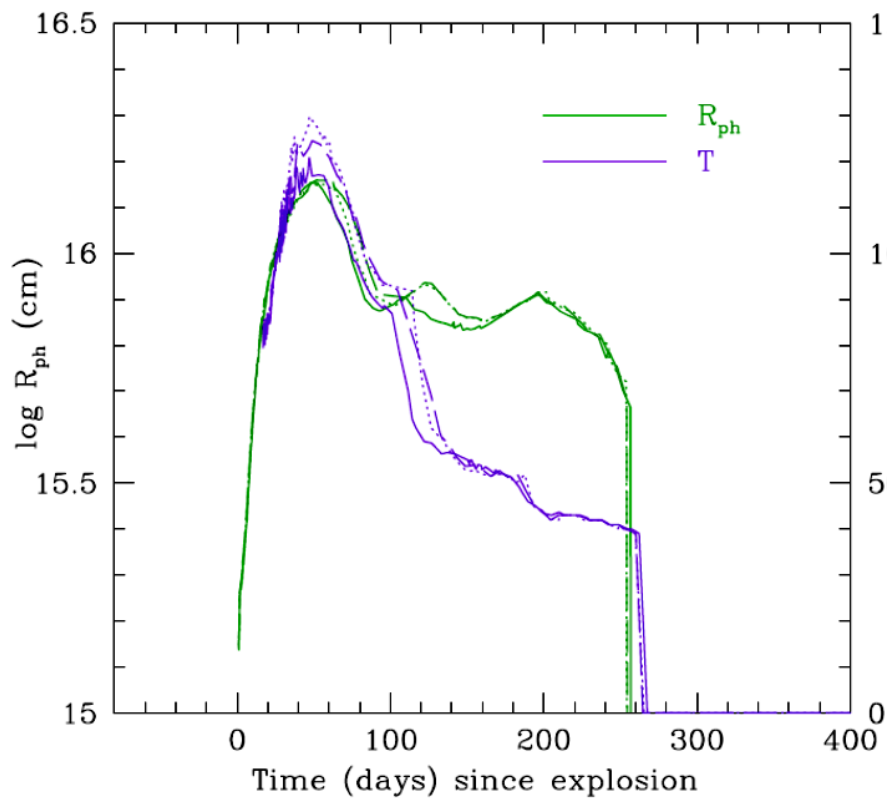


# PTF12dam R16 model. Shock wave hydro

- Emission heats the gas
- Near the peak luminosity
- After the peak luminosity
- Light curve decline (radioactive decay of  $^{56}\text{Ni}$  to  $^{56}\text{Co}$  to  $^{56}\text{Fe}$ )

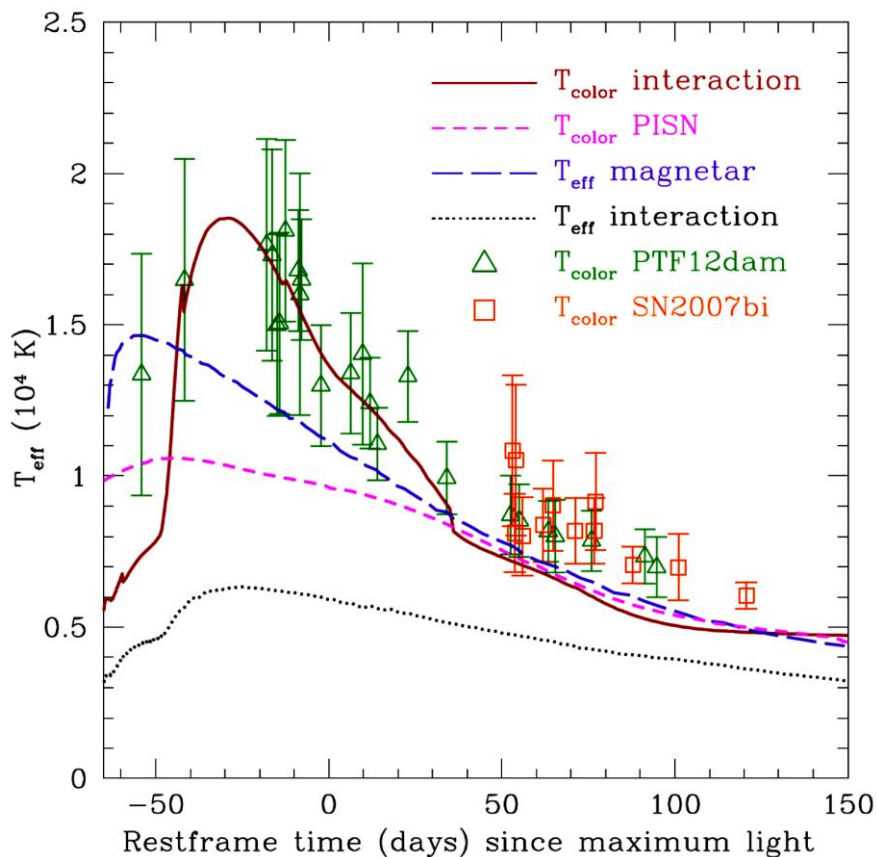


# Photospheric temperature and radius



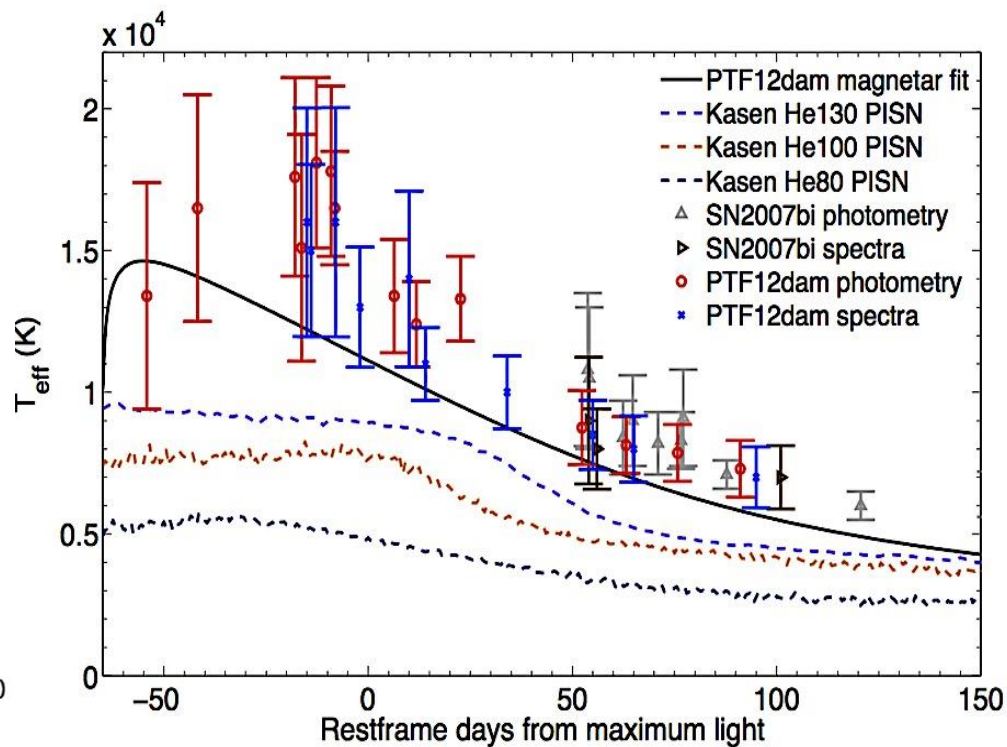
# PTF12dam R16 model. Temperature evolution

- Color and effective temperature evolution of PTF 12dam and SN 2007bi compared with interaction model

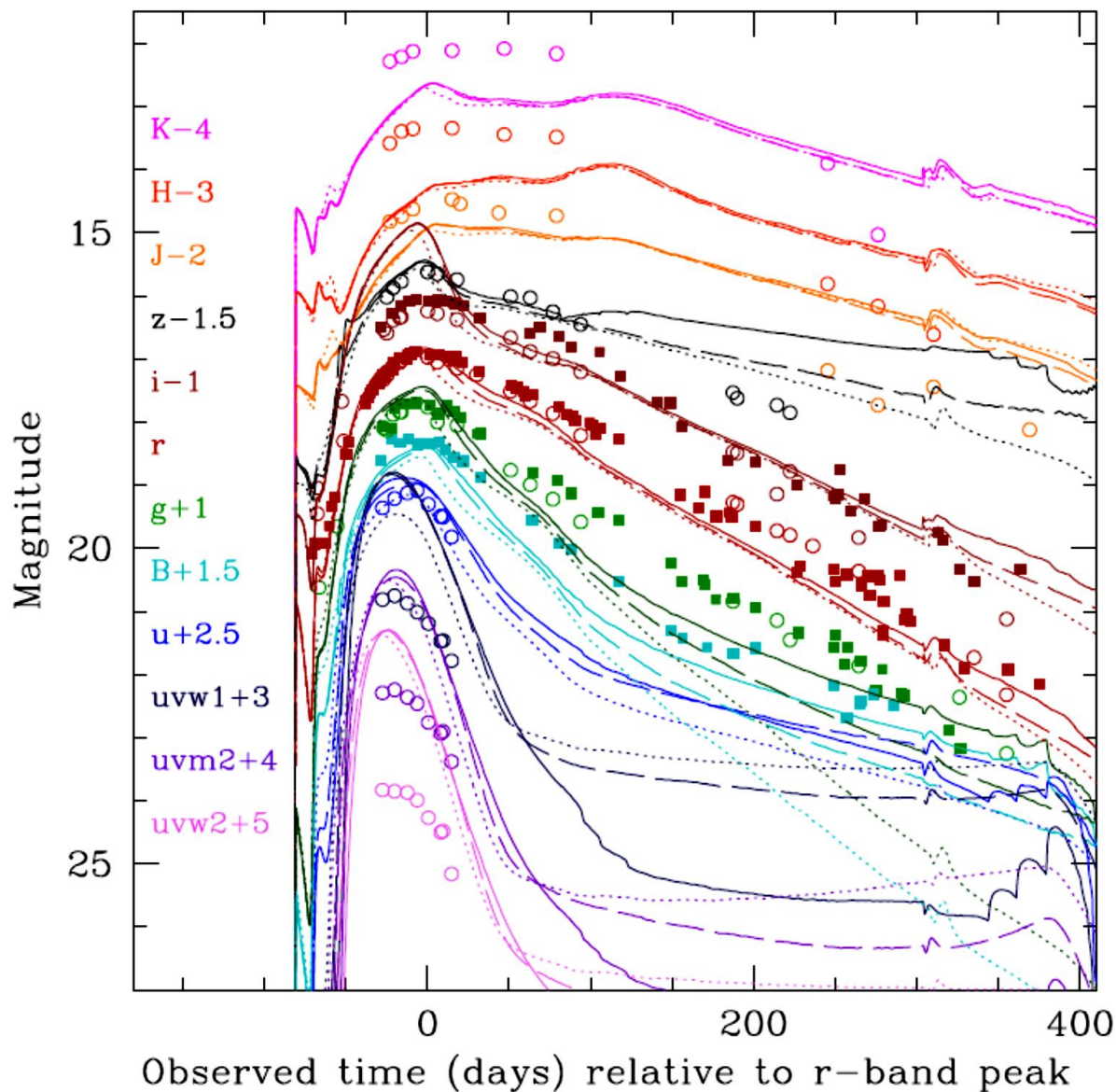


- Effective temperature evolution of PTF 12dam and SN 2007bi compared with magnetar-powered and PI models (Nicholl 2013)

- $T_{\text{color}}$  - temperature of the blackbody whose SED most closely fits the data;  
 $T_{\text{eff}} = (L/(4\pi\sigma R^2))^{1/4}$

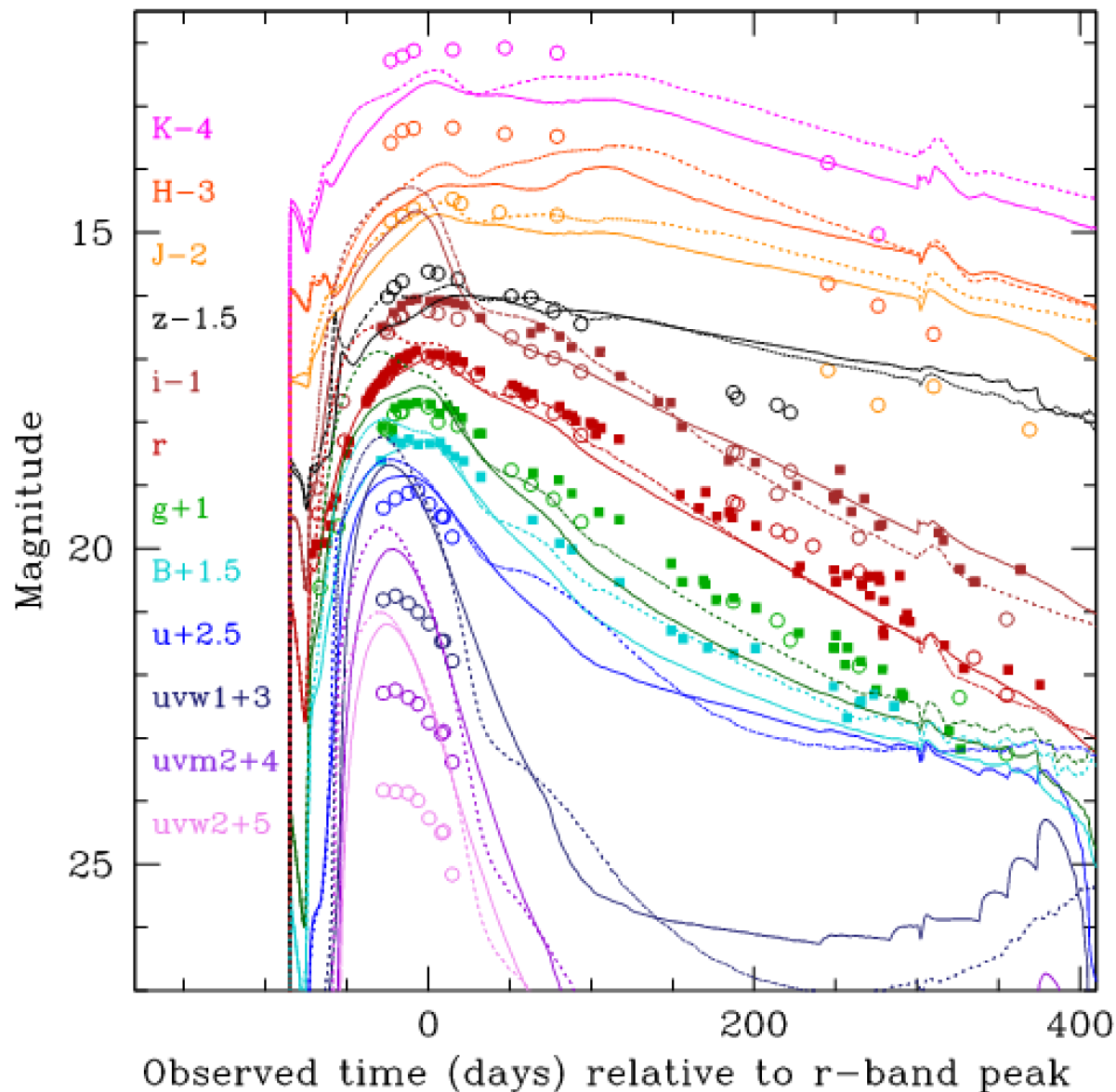


# Metallicity of CSM



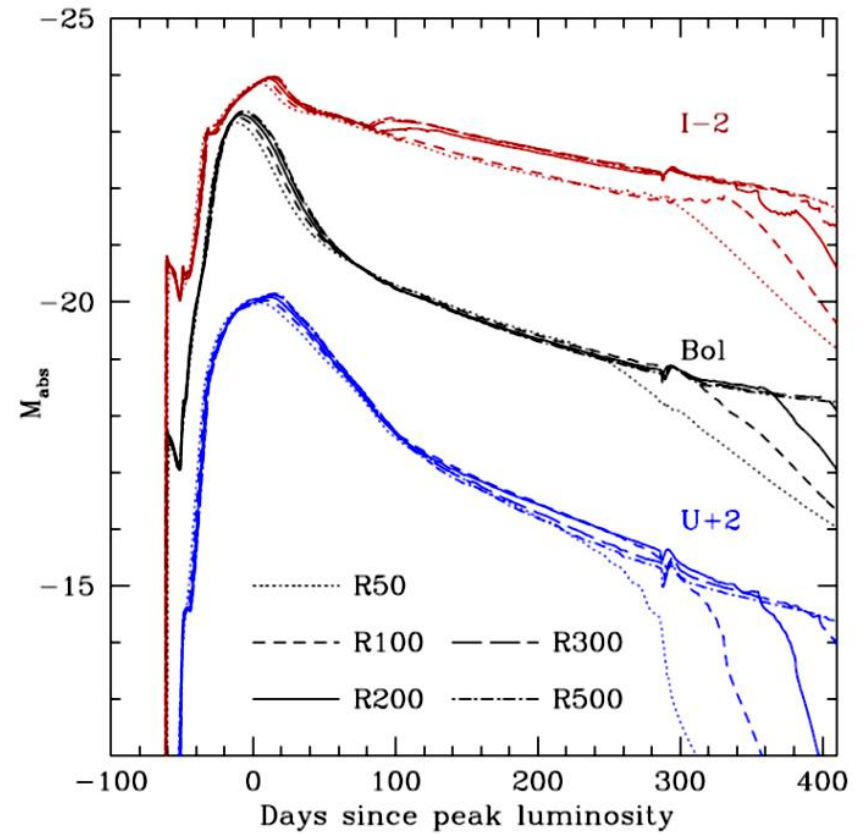
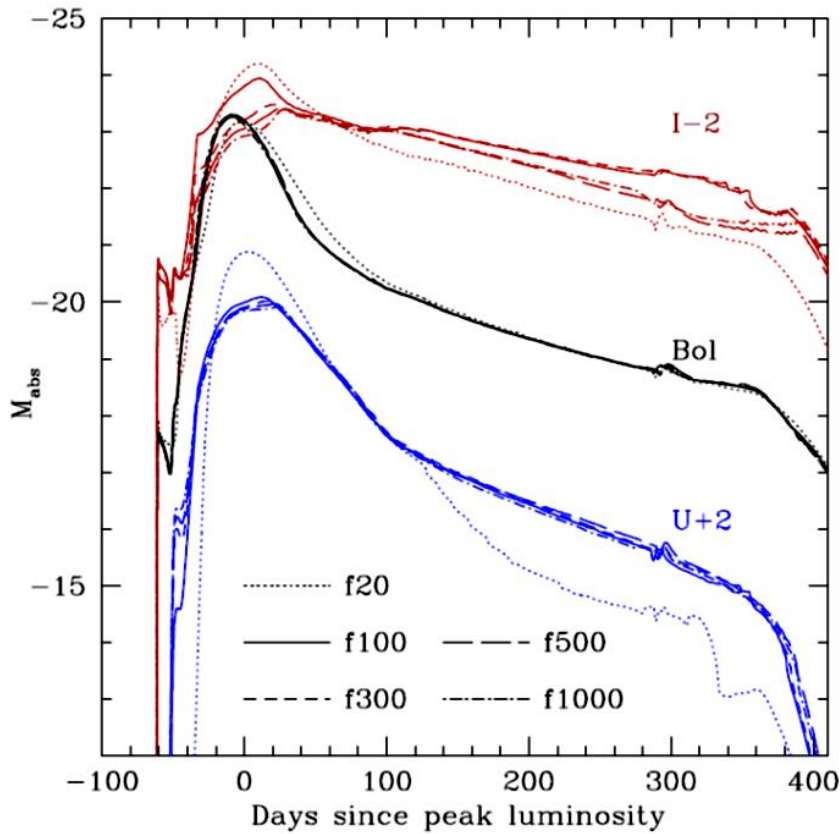
- Solar metallicity (solid line), low  $Z = Z_{\odot}/200$  (dashed line), zero metallicity (dotted line).
- Due to lower opacity, the CSM cools down faster and the optical light curve decline increases.
- The decrease of the radius of the photosphere, especially in UV wavelengths. The temperature of internal CSM layers is higher, that leads to higher luminosity at UV wavelengths.

# PTF12dam light curves. Opacity

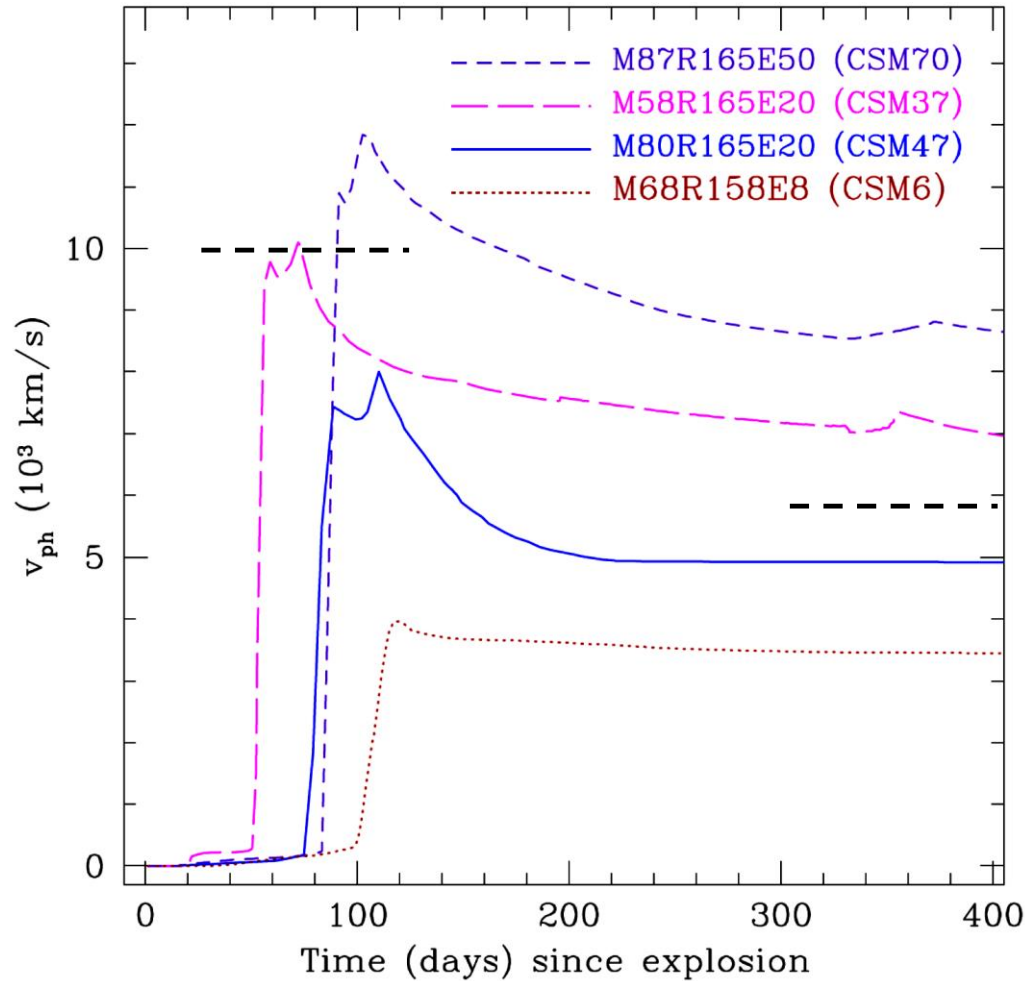


- 100,000 -> 26,000,000 lines (in prep., Sorokina 2018)
- Brighter peak in all the bands ~ 0.5 mag

# Space and energy resolution



# PTF12dam R16 model. Velocity evolution



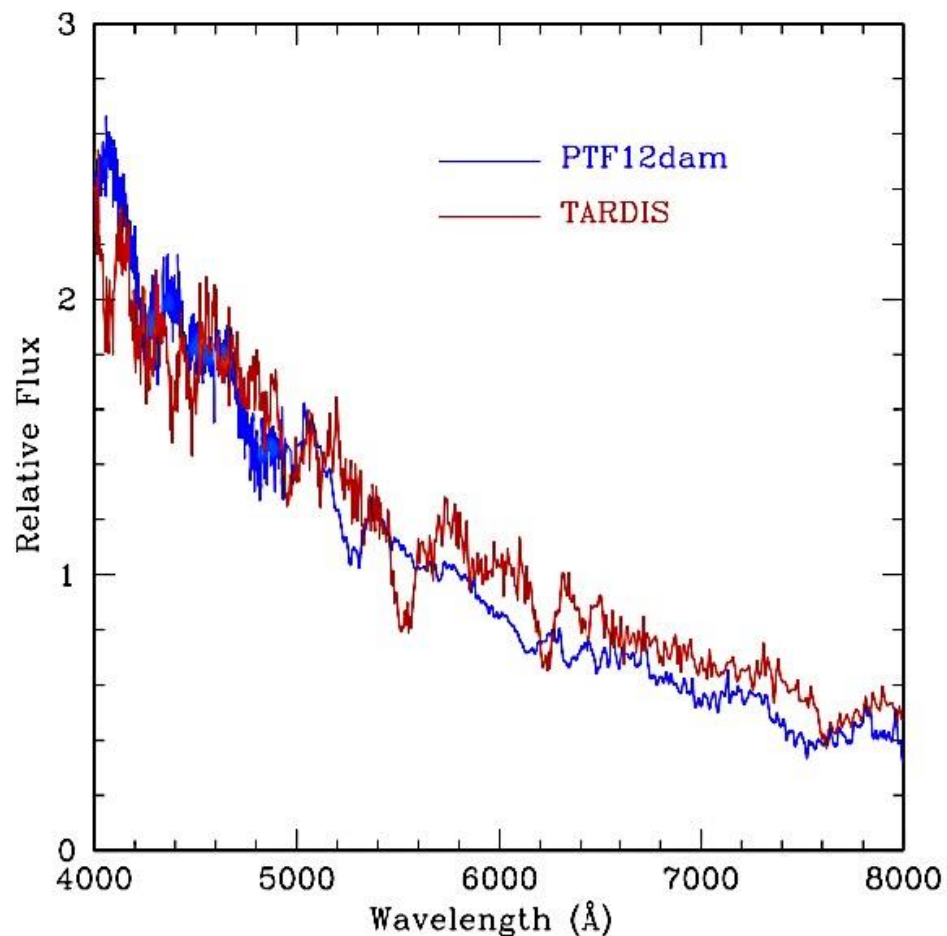
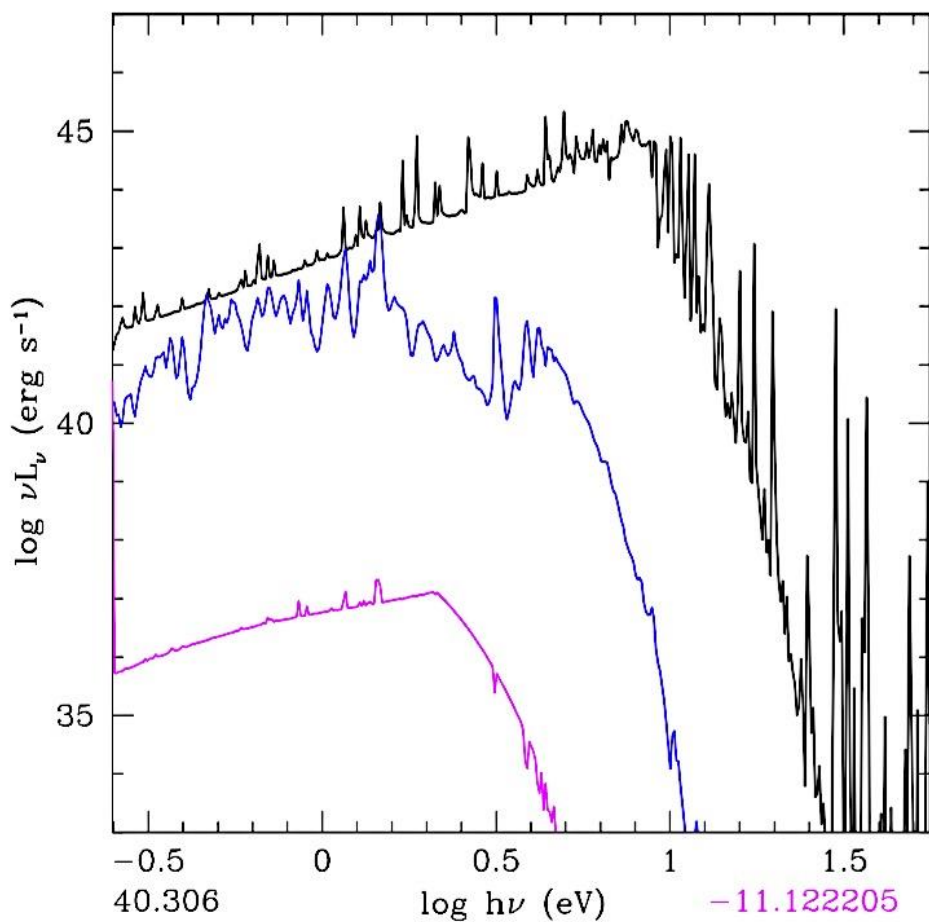
- Flux measurements of the broad SN lines of PTF12dam in the GTC spectrum taken at +509d (Chen 2014).

SN Name	Line	$\lambda$ ( $\text{\AA}$ )	Flux $\pm$ Error ( $\text{erg s}^{-1} \text{cm}^{-2}$ )
PTF12dam (+509d)	[O I]	5577	$7.0 \pm 0.5 \times 10^{-18}$
	[O I]	<b>6300 6363</b>	<b><math>4.6 \pm 0.3 \times 10^{-17}</math></b>
	[Ca II]	7291 7324	$1.1 \pm 0.1 \times 10^{-17}$
	O I	7771-7775	$1.2 \pm 0.1 \times 10^{-17}$
SN 2007bi (+470d)	[O I]	<b>6300 6363</b>	<b><math>2.4 \pm 0.3 \times 10^{-16}</math></b>
SN 2007bi (+367d)	[O I]	<b>6300 6363</b>	<b><math>6.0 \pm 0.4 \times 10^{-16}</math></b>

SN Name	EW ( $\text{\AA}$ )	FWHM ( $\text{\AA}$ )	Velocity ( $\text{km s}^{-1}$ )	Luminosity $\pm$ Error ( $\text{erg s}^{-1}$ )
PTF12dam (+509d)	187	74	$\sim 4000$	$1.9 \pm 0.2 \times 10^{38}$
	<b>332</b>	<b>137</b>	<b><math>\sim 5800</math></b>	<b><math>1.3 \pm 0.1 \times 10^{39}</math></b>
	71	102	$\sim 4000$	$2.9 \pm 0.3 \times 10^{38}$
	78	109	$\sim 4200$	$3.3 \pm 0.4 \times 10^{38}$
SN 2007bi (+470d)	<b>190</b>	<b>143</b>	<b><math>\sim 6100</math></b>	<b><math>9.5 \pm 1.0 \times 10^{39}</math></b>
SN 2007bi (+367d)	<b>358</b>	<b>182</b>	<b><math>\sim 8100</math></b>	<b><math>2.4 \pm 0.2 \times 10^{40}</math></b>

# PTF12dam R16 model. Spectral synthesis (in progress)

- STELLA run-time calculations (1000 groups): **before shock breakout**, near the peak luminosity, **+350d after maximum**
- TARDIS code (Kerzendorf & Sim 2014) post-process calculations: comparison with the observed spectrum near maximum light



# Models of Gaia16apd

- **Gaia16apd**: extremely luminous UV emission among SLSNe (Yan+17, Nicholl+17, Kangas+17).
- **Simulations**: multicolor radiation hydrodynamics. Comparison of light curves, color temperature evolution and photospheric velocities.

- **Shock interaction with CSM**

Interaction models ( $N \sim 100$ ) (Tolstov+2017):  $M_{\text{ej}} = 40 M_{\odot}$ ,  $M_{\text{CSM}} = 3 \dots 100 M_{\odot}$ ,  $\log R_{\text{CSM}} = 14 \dots 17$  cm,  $E_{51, \text{kin}} = 5 \dots 60$ , CO / He composition,  $M(^{56}\text{Ni}) = 0 \dots 6 M_{\odot}$ .

- **Magnetar pumping**

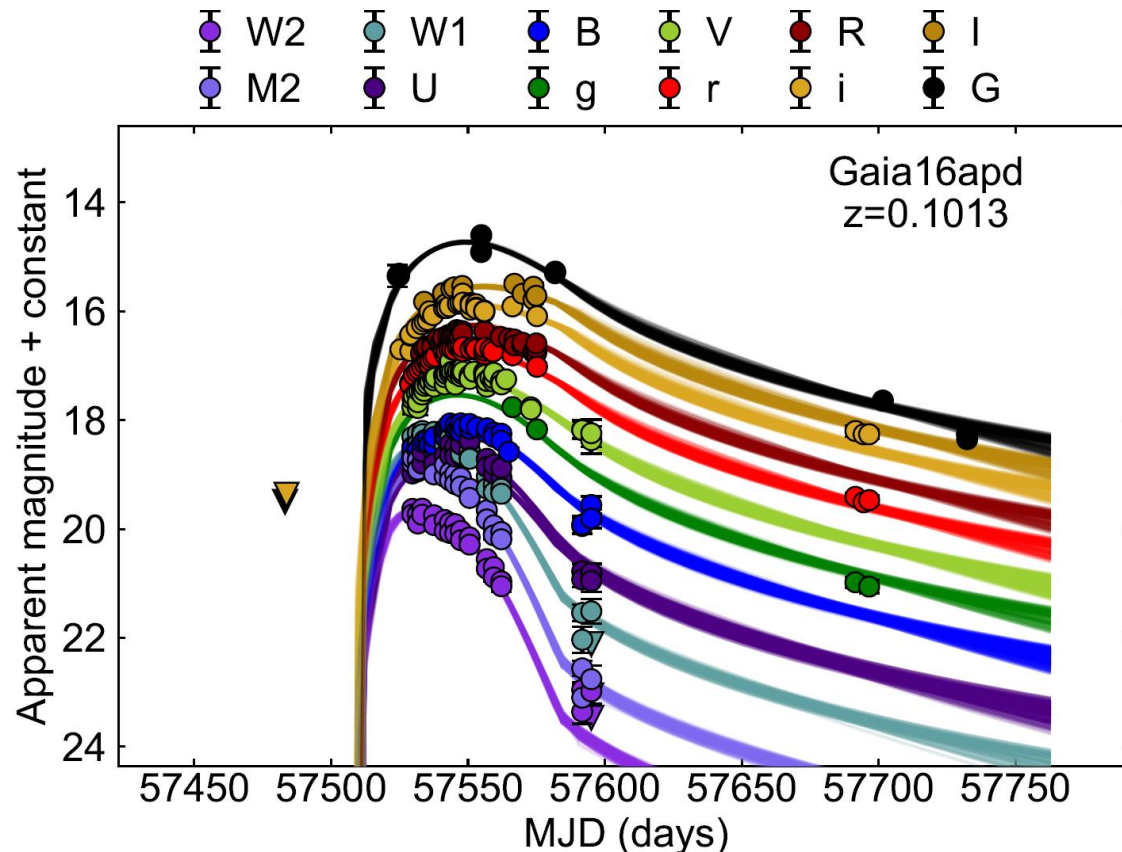
Magnetar models ( $N \sim 30$ ) constructed from SN 1998bw ejecta  $M_{\text{ej}} \sim 10 M_{\odot}$  with various magnetar parameters around  $P = 1$  ms,  $B = 10^{14}$  G.

- **Pair-instability supernova**

He130Ni55 progenitor model (Heger&Woosley 2002),  $R = 4 R_{\odot}$ ,  $M(^{56}\text{Ni}) = 55 M_{\odot}$ ,  $M = 57 M_{\odot}$ ,  $E_{51, \text{dep}} = 44$ .

# Magnetar model of Gaia16apd

- Nicholl+17, 38 SLSN-I, 12 parameters
- Magnetar parameters:  $B$ ,  $P$ ,  $M_{ej}$ ,  $\kappa$ , blackbody SED, photospheric radius expands at a constant velocity
- $M_{ej}=4M_{\odot}$ ,  $\kappa=0.2\text{cm}^2/\text{g}$ ,  $B=2\cdot 10^{14}\text{G}$ ,  $P=2.1\text{ms}$ ,  $E_{kin}= 2.4\text{foe}$



# Magnetar model

(Kasen & Bildsten 2010)

- For PISN and interaction model the energy deposition rate  $L_{\text{dep}} = E_{\text{dep}}/t_{\text{dep}}$  during  $t_{\text{dep}} \sim 0.1\text{s}$ .
- The energy deposition rate  $L_{\text{dep}}$  in magnetar model is

$$L_{\text{dep}} \sim E_{\text{dep}} / (1 + t/t_m)^2,$$

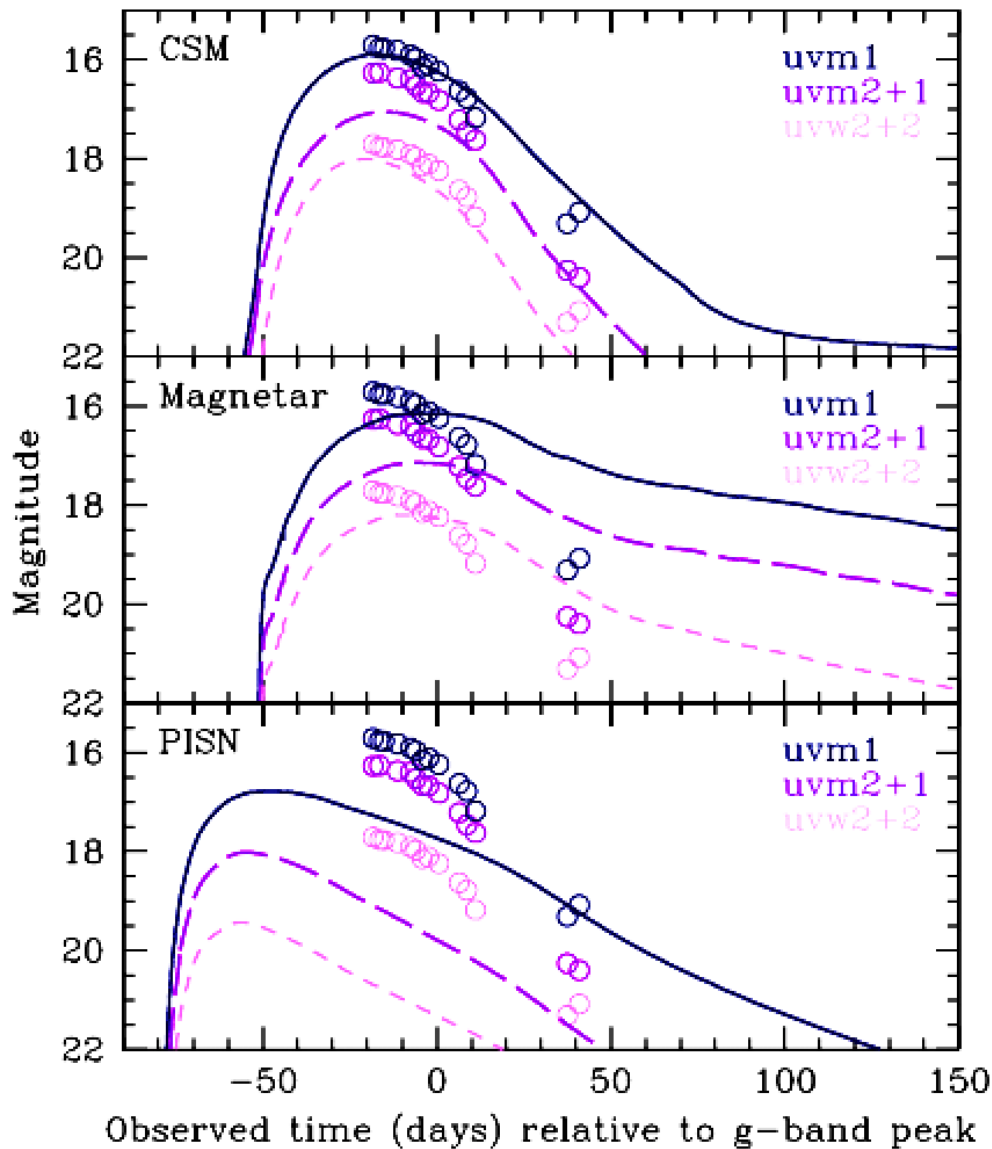
where the total spin energy  $E_m$  and spin-down timescale  $t_m$  is connected with pulsar spin period  $P$  and its magnetic field  $B$ :

$$E_m \approx 2 \times 10^{52} P_{\text{ms}} \text{ ergs},$$
$$t_m \approx 5 B_{14} P_{\text{ms}} \text{ days},$$

where  $P_{\text{ms}} = P/1 \text{ ms}$  and  $B_{14} = B/10^{14} \text{ G}$ .

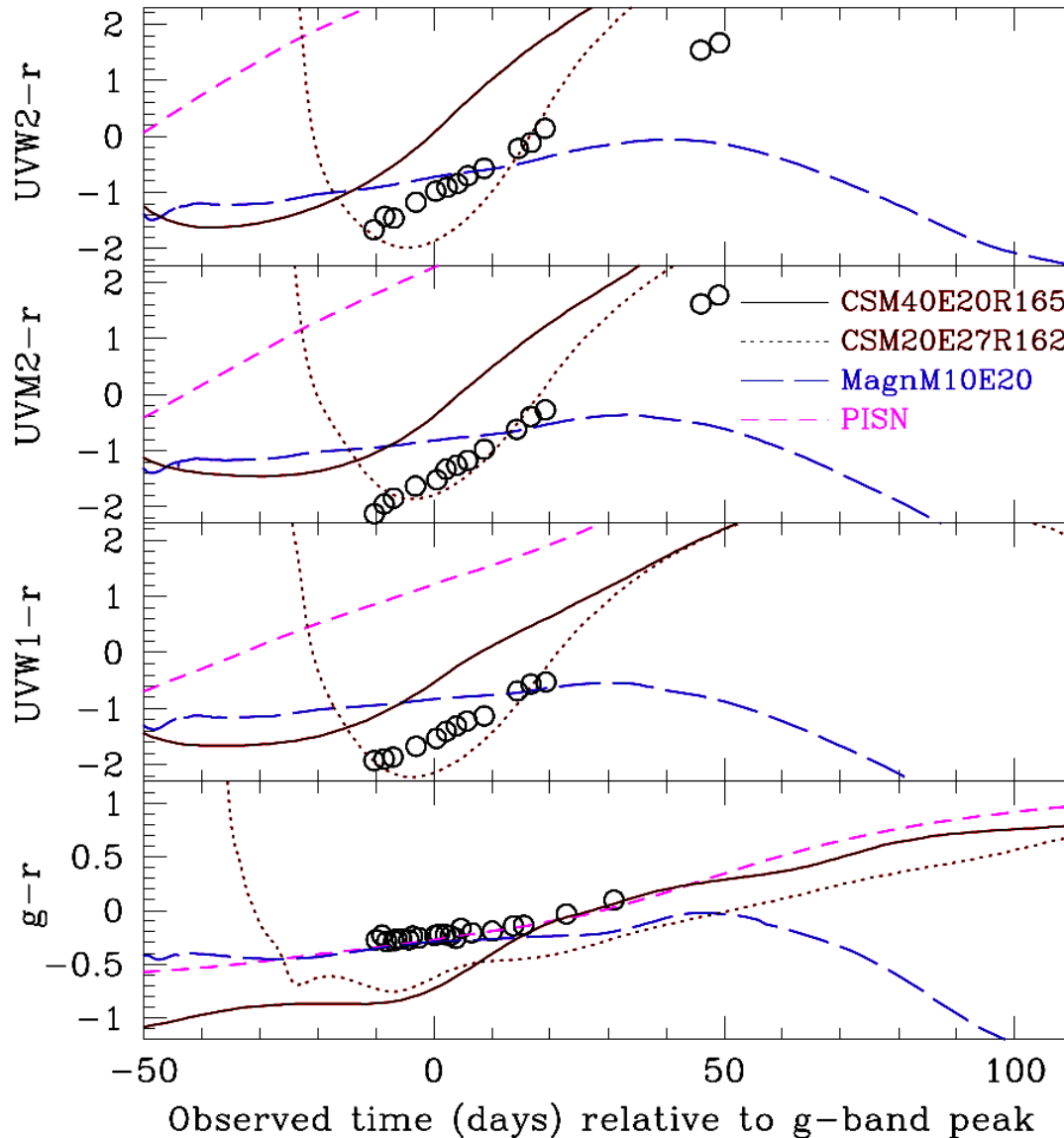
- We assume that all spin-down energy is thermalized in the ejecta.

# Ultraviolet Emission of Gaia16apd



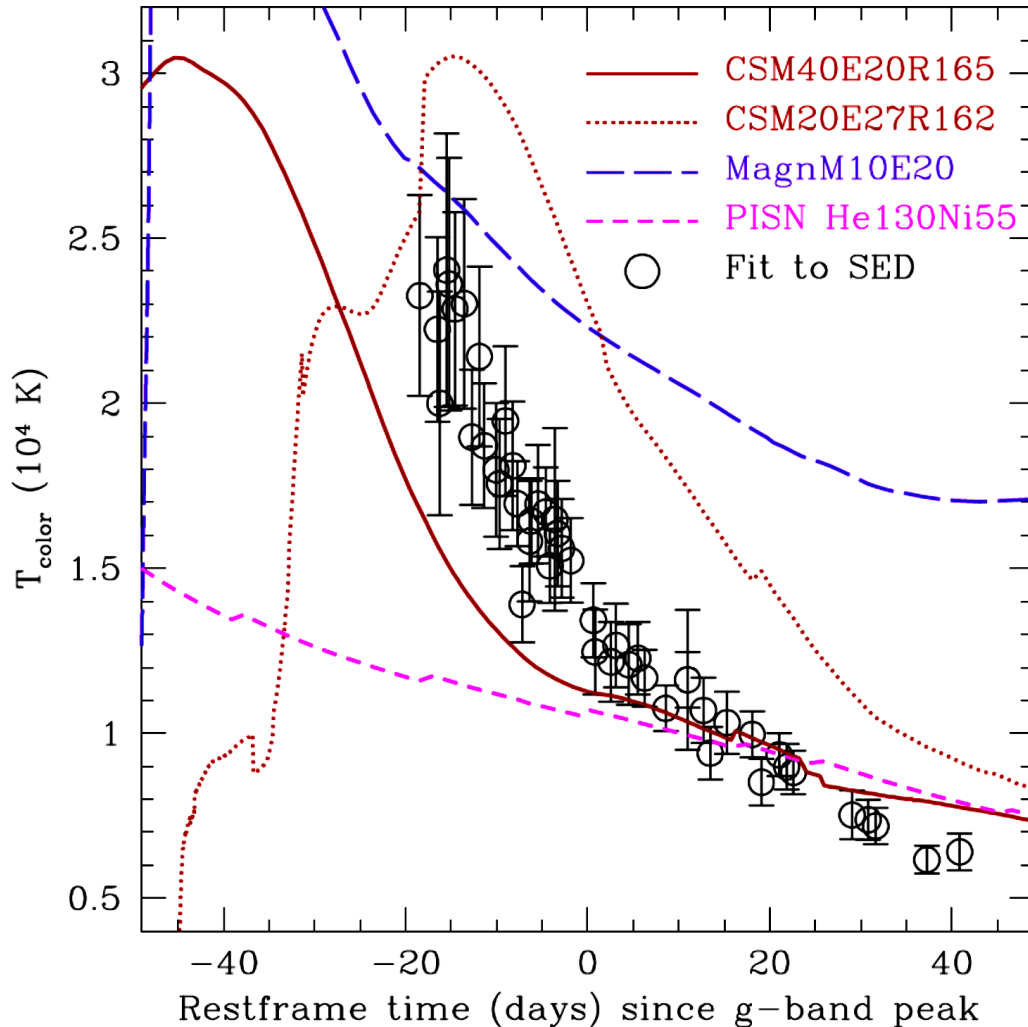
- **Which model best fits the UV data?**
  - Shock interaction with CSM
  - Magnetar pumping
  - Pair-instability supernova
- The best-fit (chi-squared minimization) of UV and optical light curves to Gaia16apd among ~ 150 models.
- **Conclusion:** interaction model is the most promising to explain extreme UV luminosity of Gaia16apd.

# Gaia16apd color evolution



- The interaction model (CO) is in better agreement with observations.
- The magnetar model has a slower reddening than observations.
- The PISN model is in good agreement with the observed reddening rate, but the model evolves about 50 days earlier than the observed one.
- g - r color evolution is more consistent with the magnetar and the PISN model.

# Gaia16apd color temperature evolution



- $T_{\text{color}}$  - temperature of the blackbody whose SED most closely fits the data;  
 $T_{\text{eff}} = (L/(4\pi\sigma R^2))^{1/4}$
- The temperature decline rate is a better fit to the observed values in interaction models
- Variation of chemical composition of CSM.
- The interaction models do not produce X-ray emission: radiation-dominated shock wave,  $T_{\text{ej}} \sim 20,000\text{-}30,000 \text{ K}$

# Summary

- We propose that **PTF12dam, Gaia16apd** are **PPISN**, where the outer envelope of a progenitor is ejected during the pulsations. UV light curves, color and temperature evolution fit the observations.
- **Parameters:**  $E_{51}=20\dots30$ ,  $M_{\text{ej+env}}=40M_{\odot}+20\dots40M_{\odot}$ ,  $M(^{56}\text{Ni})=6\dots7 M_{\odot}$ ,  $R = 10^{16}$  cm.
- **Open questions:** CO/He composition, “dark helium”, time scale of the formation of the envelope and its radius, density and temperature profiles, asymmetric explosion, velocities.
- The magnetar model requires more detailed simulations of high-energy effects: pair-productions, spectral transport of gamma-rays, inverse Compton, coupling of wind and plasma.
- Combined multicolor light curve and spectra modeling are required to identify the scenario of SLSNe, parameters of supernovae (E, M, Z).